

The resonant interaction of disturbances at laminar–turbulent transition in a boundary layer

By YU. S. KACHANOV AND V. YA. LEVCHENKO

Institute of Theoretical and Applied Mechanics, Siberian Branch of the U.S.S.R. Academy of Sciences, Novosibirsk, U.S.S.R.

(Received 26 January 1983 and in revised form 26 August 1983)

The three-dimensional resonant interaction of a plane Tollmien–Schlichting wave, having a frequency f_1 , with a pair of oblique waves having frequencies $\frac{1}{2}f_1$, was observed and studied experimentally. In the initial stages, the interaction proved to be a parametric resonance, resulting in the amplification of small random priming (background) oscillations of frequency $\frac{1}{2}f_1$, and of a packet of low-frequency oscillations. The resonant interaction of waves in a boundary layer was investigated also by introducing a priming oscillation with frequency $f' = \frac{1}{2}f_1 + \Delta f$ for different values of the frequency detuning Δf . The importance of the discovered wave interaction in boundary-layer transition is demonstrated. Causes of realization of different types of laminar-flow breakdown are discussed.

1. Introduction

Much theoretical and experimental work has been devoted to the study of the physical nature of the laminar–turbulent transition phenomenon. The state of the art for this problem is adequately described in Eppler & Fasel (1980).

Transition can be fruitfully studied by means of experimental modelling of the relevant complex wave phenomena taking place during this process. This permits (1) the separation of different processes in more or less pure form; (2) the comparison of theoretical models with such processes; and (3) the tracing of sequences of such processes and phenomena, thus drawing nearer to an understanding of the process of transition to the turbulent regime. Developed in the pioneering work of Schubauer & Sramstad (1947), the method of the vibrating ribbon is one of the main methods for obtaining controlled conditions for the development of disturbances in boundary layers and in other shear flows (see e.g. the experiments of Nishioka, Iida & Ishikawa 1975; Kozlov & Ramazanov 1981). As a packet of Tollmien–Schlichting waves, observed in ‘natural’ transition in a Blasius boundary layer (Schubauer & Sramstad 1947), was modelled by a two-dimensional harmonic wave in the work of Klebanoff & Tidstrom (1959) and Kachanov, Kozlov & Levchenko (1977), fast development of three-dimensionality of both the disturbance fields and mean flow was discovered as an integral part of the laminar-flow breakdown process. A more accurate definition of the experimental model with the introduction of a controlled three-dimensionality into a boundary layer, which had been made by Klebanoff, Tidstrom & Sargent (1962), Tani & Komoda (1962), Hama & Nutant (1963) and Komoda (1967), gave the possibility of studying the process of the subsequent development of disturbances and mean flow at transition to turbulence. Unfortunately, the reasons for the initial three-dimensionality remains undetermined. Various theoretical models (a good review is given in Craik 1980), prognosticating physically

likely mechanisms for the onset of three-dimensionality, have not been validated because of the lack of sufficiently detailed experimental data for their approbation. Theoreticians have to use the pioneering experiments by Klebanoff & Tidstrom (1959) and Klebanoff *et al.* (1962). These experiments gave detailed information on the development of disturbances at transition to turbulence, which, however, had to do with a later stage – the stage of a formed three-dimensionality. Moreover, unfortunately, a dearth of spectral analysis is present in these works. Therefore a comparison of theoretical results (in particular, in the works of Craik 1980; Nayfeh & Bozatlı 1979*b*) with the experimental data has an only qualitative nature.

On the other hand it is impossible to consider that the question on paths of the randomization of the disturbances development process has been solved. The randomization in free shear layers (jets, wakes, mixing layers) takes place apparently by means of successive excitations of higher harmonics, in some cases subharmonics, and the generation of combination modes (see Sato 1960; Sato & Kuriki 1961; Freymuth 1966; Miksad 1972, 1973). Such a type of transition was called an evolutionary transition, in contrast with the ‘catastrophic’ breakdown of the laminar regime which is inherent to wall streams, in particular to boundary layers. The detailed description of the last type of transition has been established by the classical experiments of Klebanoff & Tidstrom and Klebanoff *et al.* (1962). This type of breakdown is characterized by the sudden appearance of ‘spikes’ in the oscilloscope traces of the streamwise velocity signal and by a subsequent generation of packets of high-frequency oscillations in each period of a fundamental wave, eventually developing to turbulent spots. In view of the detailed description of such a type of transition to turbulence in the work of Klebanoff *et al.* (1962), it is possible, following Herbert & Morkovin (1980), to name it the K-type breakdown of a laminar regime or, briefly, by K-breakdown. The appearance of bursts of high-frequency oscillations has been called the secondary instability phenomenon. If theoretical models of the onset of three-dimensionality are not supported by experiment, the case of the high-frequency secondary instability is somewhat different. In spite of available experimental data in the works of Klebanoff & Tidstrom and Klebanoff *et al.* (1962), Kovasznay, Komoda & Vasudeva (1962) etc. theoretical studies of this phenomenon (see Betchov 1960; Greenspan & Benney 1963; Gertsenshtein 1969; Landahl 1972; Zhigulyov *et al.* 1976, Zelman 1981; Itoh 1981) have a qualitative nature in view of the strong nonlinearity and three-dimensionality of the process.

However, the K-breakdown regime is not the universal path of turbulence onset in boundary layers. In particular, Komoda (1967) and Kachanov *et al.* (1977) found that the transition in a boundary layer can take place without high-frequency bursts and turbulent spots. Kachanov, Kozlov & Levchenko (1980) showed how a low-frequency intermittency and turbulent spots can appear, the secondary instability mechanism not being invoked to explain their appearance. The transition process in the work of Kachanov *et al.* (1977), besides absence of the intermittency, had other features of the evolutionary type of transition. For instance, for the first time the excitation of the subharmonic was discovered in a wall boundary layer. The appearance of some low-frequency fluctuations was also registered. This was also observed by Saric & Reynolds (1980). These fluctuations, together with the subharmonic, played a large role in the process of the flow randomization, being a kind of trigger mechanism for the beginning of the invasion of the spectrum into the region of high frequencies and for the breakdown of the laminar regime. It was supposed by Kachanov *et al.* (1977) that a three-wave interaction (see Raetz 1959; Craik 1971;

Volodin & Zelman 1978) had been the reason for the subharmonic excitation. Rabinovich (1978) had supposed that low-frequency fluctuations, observed by Kachanov *et al.* (1977), might be amplified owing to the modulation instability phenomenon (see Whitham 1974). However, these hypotheses were not factually based. Furthermore, it was mentioned by Kachanov *et al.* (1977) that these fluctuations and the subharmonic had appeared simultaneously with the onset of three-dimensionality. This fact hints at their important role in the process of the beginning of three-dimensionality.

This paper is devoted to the experimental study of the subharmonic excitation process in a laminar boundary layer at transition, initiated by an initially two-dimensional Tollmien–Schlichting wave with a frequency f_1 . The results of the investigation lead to an explanation for the excitation of low-frequency fluctuations with frequencies incommensurable with a fundamental wave frequency, and therefore give an explanation of one of the paths of flow randomization.

2. Experimental procedures

2.1. Experimental facilities

The experiments were conducted in the ITPM low-turbulence wind tunnel at freestream speed 9.18 m/s and turbulence level less than 0.02%. The wind tunnel has a 4 m long test section with a 1 m × 1 m cross-section. A flat plate having a chord length of 1.5 m, a span of 1.0 m and a thickness of 10 mm was used. The leading edge was composed of two conjugate semiellipses with axis of 2 mm:132 mm on the working side of the plate and of 8 mm:132 mm on the opposite side. The flat plate was mounted in the test section horizontally under zero angle of attack. Beginning at $x = 100$ mm from the leading edge, the pressure gradient was not more than 0.8% per 1 m of length, i.e. the model had essentially a zero pressure gradient, except for a region near the leading edge.

Sinusoidal disturbances (Tollmien–Schlichting waves) were introduced into the laminar boundary layer by a vibrating ribbon 0.05 mm thick and 3 mm wide with the unsupported span of 300 mm. The ribbon was located 250 mm downstream of the leading edge at a height of 0.15–0.2 mm from the plate surface.

2.2. Recording and processing of data

Development of wave disturbances in a boundary layer and the structure of a mean flow were recorded by the use of one or two hot-wire anemometer probes. The wires were Wollaston with 6 μm diameter of platinum core and sensitive wire length of 0.5 mm. The signals were conditioned using a DISA 55D01 hot-wire anemometer with the linearizer. The basic scheme of data recording is given in figure 1(a). Constant and variable components of a signal from the first probe, a signal from the second probe and a reference signal (from the sine signal generator) were recorded, at all principal measurements, on four channels of a seven-channel tape recorder in the regime of frequency modulation, with the following signal processing.

A typical scheme of signal processing for reproducing tape records is represented in figure 1(b). This scheme was applied for measurements of distributions of spectral components versus the space coordinates, for comparison of signals from the different probes, and for the measurement of a flow mean velocity (constant voltage). The frequency spectra were obtained using a different scheme. Beforehand, the record

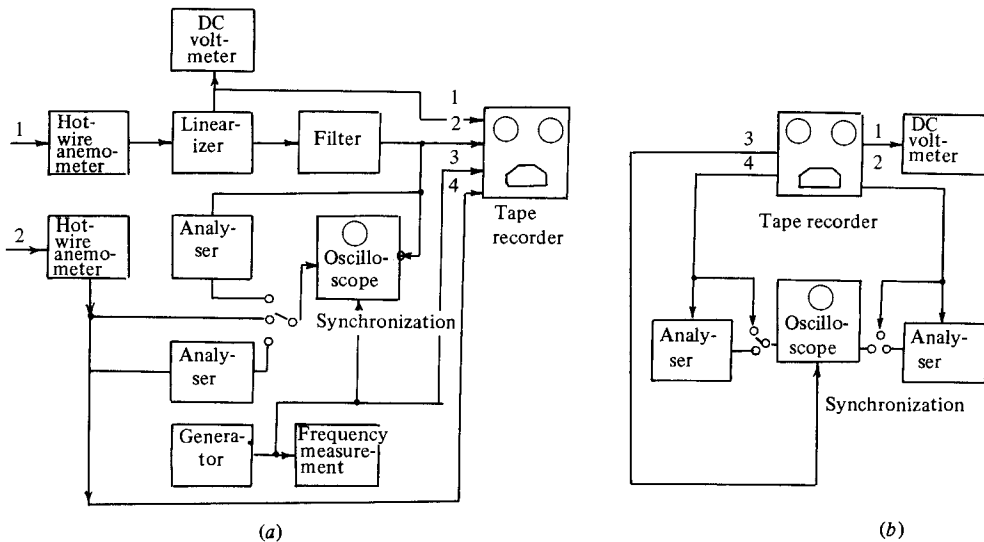


FIGURE 1. Schematic of registration (a) and processing (b) of signals.

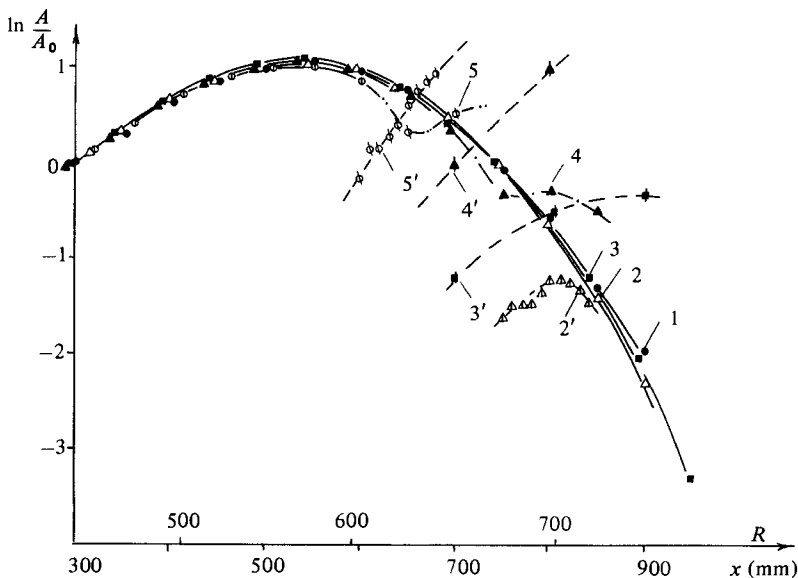


FIGURE 2. Amplification curves for the fundamental waves (1, 2, 3, 4, 5) and corresponding subharmonics (2', 3', 4', 5') at different initial amplitudes of a fundamental wave: $A_0 = 0.022; 0.163; 0.218; 0.436$ and 0.654% . $f_1 = 120$ Hz, $F_1 = 137 \times 10^{-6}$.

segment, corresponding to the measurement in the given point of the flow, was rerecorded on a second tape recorder supplied by a ring tape. After that, the record was reproduced during the time needed for conducting of spectral analysis in the regime of scanning of the analyser spectral window on a centre frequency. Recording of the spectrum was made by an (x, y) -recorder at 5 s averaging times in analyser output and 4 Hz bandwidth.

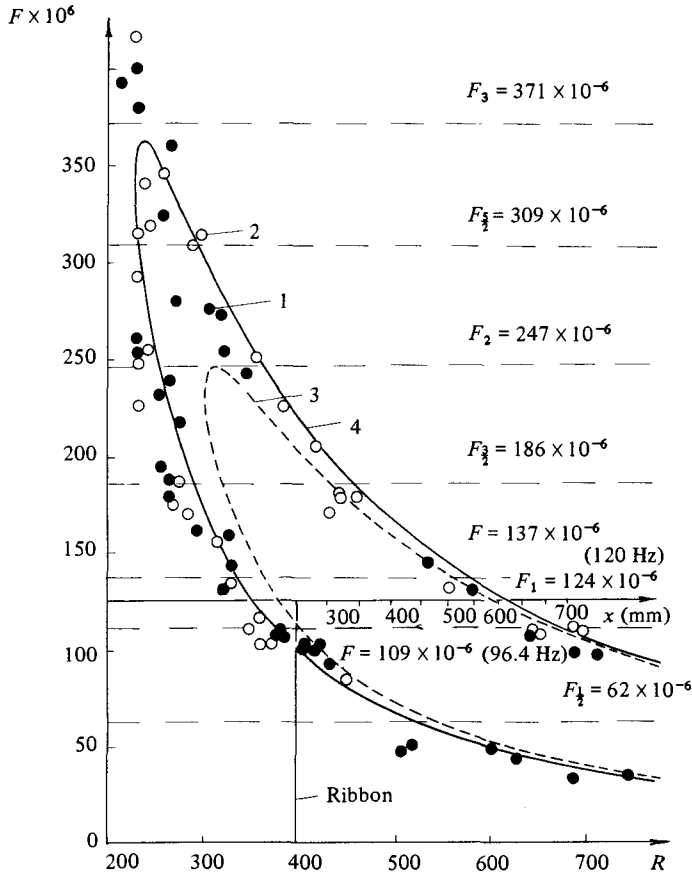


FIGURE 3. Measurement regions with respect to the stability diagram. 1, 2, experiments by Ross *et al.* (1970) and Kachanov *et al.* (1974); 3, 4, parallel and non-parallel theory of Saric & Nayfeh (1975).

3. Resonance excitation of subharmonics from natural disturbance

3.1. The choice of a measurement regime

During the preliminary stage of the experiments, a study was made of a range of amplitudes of waves introduced by the vibrating ribbon as the type of transition discovered by Kachanov *et al.* (1977) took place. This type of transition is characterized by a low-frequency breakdown of a laminar flow (without formation of turbulent spots) through excitation of a subharmonic wave and incommensurable low-frequency fluctuations and by the filling of the spectrum as a result of a nonlinear interaction of high- and low-frequency disturbances.

Streamwise distributions of amplitudes of the fundamental wave with the frequency $f_1 = 120$ Hz ($F = 137 \times 10^{-6}$) and oscillations with the frequency $f_{\frac{1}{2}} = 60$ Hz at different initial amplitudes of the fundamental wave are given in figure 2. The position of the regions of frequency parameters and Reynolds numbers under investigation is shown in figure 3, where the neutral stability curve for a Blasius boundary layer is taken from the work of Saric & Nayfeh (1975). The amplitudes of harmonics had been measured at y -positions corresponding to maxima in their y -distributions. The recording of subharmonics was made only when their amplitudes approached the

amplitudes of a fundamental wave. It was observed for the first time in the regime as $A_0 = 0.163\%$. In this case the amplitudes of harmonics were only about 0.05% . At larger initial amplitudes A_0 the subharmonic overtakes the fundamental wave, and at approximately the same place a change of the amplification rate of the fundamental wave takes place. Normal-to-the-wall profiles of the fundamental wave are transformed and their form becomes like a bell with a maximum placed far from the wall (see also Kachanov *et al.* 1977). A packet of low-frequency oscillations ($f < f_1$) grows together with the subharmonic. Its appearance signals the onset of a process of the laminar-flow breakdown (also see Kachanov *et al.* 1977). Analogous results were obtained for the frequency $f_1 = 96.4$ Hz ($F = 2\pi f\nu/u_\infty^2 = 113 \times 10^{-6}$).

It should be mentioned that, for all cases studied, the oscillations with a frequency $f_{\frac{3}{2}}$ had reached considerable amplitudes $A_{\frac{3}{2}} \sim A_1$ only in the region of the second branch of the neutral curve and behind it.

As an initial amplitude A_0 of the fundamental wave approached 1% (its amplitude in the region of the second branch of the neutral curve approached $2.5\text{--}3\%$ at $f_1 = 120$ Hz in these experiments), the higher harmonics were excited and grew intensively from the very beginning of the measurement region ($x \geq 300$ mm). At the same time the three-dimensionality of both fluctuations and the mean flow became stronger, and the regime of K-breakdown of a laminar flow (see Klebanoff & Tidstrom 1959 and Klebanoff *et al.* 1962) with typical 'spikes' in the oscilloscope traces and other phenomena arose. This quite different type of breakdown is a subject of special investigations. In just this sense the principal investigations of this paper were carried out at not too large values of initial amplitudes of disturbances, which corresponded approximately to ones in the work of Kachanov *et al.* (1977).

The experiments were conducted mainly in two regimes of measurements corresponding to two frequencies of the fundamental wave $f_1 = 111.4$ Hz (the principal regime) and $f_1 = 96.4$ Hz, at a freestream velocity $U_\infty = 9.18$ m/s, at distances downstream from the leading edge between $x = 300$ mm and $x = 760$ mm. These values corresponded to frequency parameters $F = 124 \times 10^{-6}$ and $F = 109 \times 10^{-6}$ and Reynolds numbers $R = Re_x^{\frac{1}{2}} = (R_\infty x/\nu)^{\frac{1}{2}} = 430\text{--}684$ (see figure 3). Thus the dimensional values of disturbance frequencies and a freestream velocity were chosen the same as those in the works of Kachanov *et al.* (1977, 1980) and Gilyov, Kachanov & Kozlov (1981).†

At the 'initial' section $x = 300$ mm ($Re = 430$), at $y/\delta = 0.26$ (i.e. approximately in the region of a maximum amplitude of the fundamental wave), in the principal regime of measurements ($f_1 = 111.4$ Hz, $F = 124 \times 10^{-6}$) the amplitude of the fundamental wave was $A_1 = (u'^2)^{\frac{1}{2}}/U_\infty = 0.62\%$, the amplitude of the second harmonic with the frequency $2f_1$ was $A_2 = 0.0118\%$, and the amplitude of the third harmonic $3f_1$ was $A_3 = 0.0007\%$. The boundary-layer thickness was determined experimentally from the condition $U/U_\infty = 0.99$. The fluctuations with frequencies $3f_1, 4f_1, \dots$ were random fluctuations having no definite phases, i.e. they were some background fluctuations having no connection with the fundamental wave. Their amplitudes in this point were not changed practically by switching off a fundamental frequency signal fed to the vibration ribbon. As in the work of Kachanov *et al.* (1977), maxima of higher-harmonic amplitudes were observed near the wall at $y/\delta \approx 0.05$, and their maximum values were at this position slightly higher, namely $A_2 = 0.035\%$ and

† In the experimental work of Gilyov *et al.* they obtained data on wavenumbers and phase velocities of a fan of oblique waves at the frequency 55 Hz which coincide with the subharmonic frequency at the principal regime ($f_1 = 111.4$ Hz) of this paper.

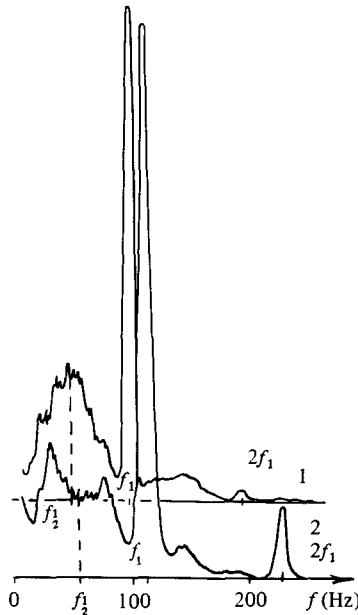


FIGURE 4. Spectra of fluctuations in the transition region at appearance of low frequencies; $y/\delta = 0.26$: 1, $f_1 = 96.4$ Hz ($F_1 = 109 \times 10^{-6}$), $x = 600$ mm ($R = 608$); 2, $f_1 = 111.4$ Hz ($F_1 = 124 \times 10^{-6}$), $x = 640$ mm ($R = 633$).

$A_3 = 0.0027\%$. However, they were sufficiently small, and apparently had no influence on the process of the subharmonic excitation under the investigation (see §4.5).

3.2. Analysis of oscillation oscilloscope traces

In these experiments as well as in the experiments by Kachanov *et al.* (1977), the essential breakdown of a laminar flow had started with the appearance of diffused low-frequency peaks, including the subharmonic, in the amplitude spectrum. At that stage a low-frequency vibration of a whole periodic, stationary, near-sine curve was observed on the oscilloscope screen at synchronization of the signal from a reference signal fed to the vibrating ribbon. The amplitude spectra of fluctuations in this region are presented in figure 4 for two different frequencies of the fundamental wave $f_1 = 96.4$ Hz ($F = 109 \times 10^{-6}$) and $f_1 = 111.4$ Hz ($F = 124 \times 10^{-6}$). In both cases the spectrum of low-frequency fluctuations ($f < f_1$) is very broad. In the case of $f_1 = 96.4$ Hz the frequency of the maximum of a packet coincides with the subharmonic f_3 , and in the case of $f_1 = 111.4$ Hz the peaks $f^* \approx 34$ Hz and $f^{**} \approx 77$ Hz are observed. In both cases the combination peaks with the frequencies $f_1 - f^*$, $f_1 + f^*$, $2f_1 - f^*$ are observed.

Amplitude spectra like those given in figure 4 definitely point out the excitation of low-frequency fluctuations, indicate the appearance of the subharmonic (see also Kachanov *et al.* 1977) and give information on the development of these disturbances. However, these spectra, of course, are not sufficient for an analysis of the causes of the excitation of subharmonics and other low-frequency oscillations. Therefore an investigation was undertaken of the phase structure of low-frequency fluctuations (of spectral-component phases) on the basis of the analysis of the oscilloscope traces obtained at the output of the frequency filter with a narrow bandwidth. Phase

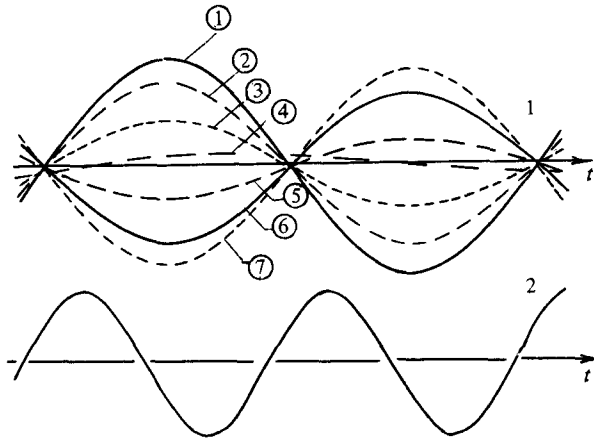


FIGURE 5. Variation of amplitude and jumps of phase of a subharmonic (1), with respect to reference signal (2), with the slow time for 7 'moments'. Bandwidth is 4 Hz; $x = 640$ mm ($R = 628$); $y/\delta = 0.26$; $z = -2.5$ mm.

correlations between these fluctuations and the fundamental wave are of the greatest interest. They can have a definite value only for some spectral components. The investigation showed that spectral components with frequencies $f_{\frac{1}{2}} = \frac{1}{2}f_1$, $f_{\frac{2}{3}} = \frac{2}{3}f_1$ and $f_{\frac{5}{3}} = \frac{5}{3}f_1$ have such correlations, invariable during the observation (several hours). In other words, these components proved to be coherent with the fundamental wave. Of course, the nature of the subharmonics, i.e. of the oscillations with the frequencies of $f_{\frac{1}{2}}$, are of greatest interest, because others are the result of the nonlinear interaction between $f_{\frac{1}{2}}$ and f_1 , $2f_1$, $3f_1$.

The oscilloscope traces of the subharmonic oscillations (in the 4 Hz bandwidth) are presented in figure 5. They were obtained at a fixed position of the probe in the region where low-frequency fluctuations were large enough. The curves 1, 2, ..., 7 correspond to seven moments of 'slow' time T . The time T is slow in the sense that ΔT (that is an interval between the i -moment and the $(i+1)$ -moment) is equal to $nT_{\frac{1}{2}}$, $n \geq 1$, where $T_{\frac{1}{2}}$ is the subharmonic period.

The introduction of two timescales permits one to operate with concepts of the amplitude and phase as the characteristics obtained with some averaging in times ΔT and to speak about changes of these characteristics with a (slow) time. The curves in figure 5 correspond to those observed on the oscilloscope screen. Figure 6(a) shows the oscilloscope traces in a unified timescale.

It is seen that a subharmonic amplitude changes continuously and its phase remains practically constant between its 180° jumps. The phase jumps take place when the amplitude crosses its zero value.†

The characteristic picture of the change of a subharmonic amplitude and phase is possible at the amplification of small background 'priming' subharmonic oscillations, whose amplitudes and phases change randomly in the time, by means of the parametric resonant interaction with the fundamental wave. Indeed, the parametric resonance has the property that the resonance amplification takes place only in the case when 'priming' oscillations (i.e. oscillations determining initial conditions for the

† As a matter of fact, some background fluctuations, whose phases have no definite values, become considerable in the region where the phase changes its value (intervals of time A , B in figure 6).

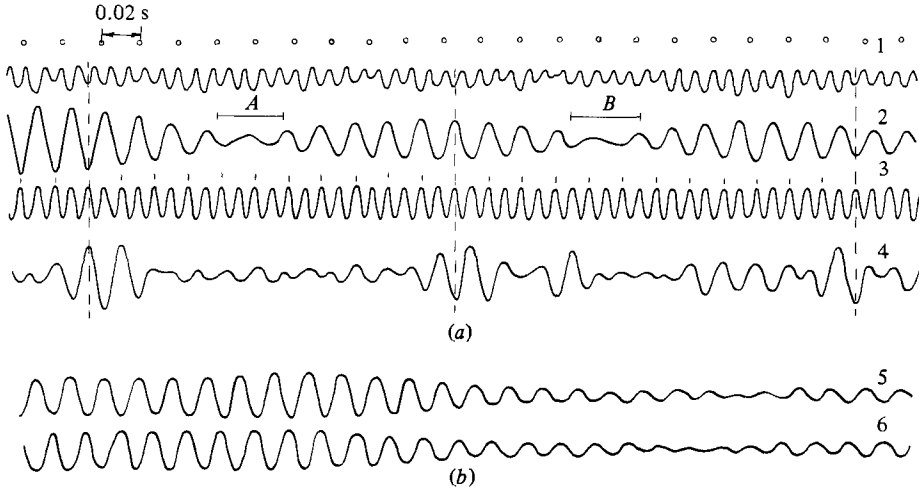


FIGURE 6. Oscilloscope traces in unified timescale. (a) (1), total signal; subharmonic signal in 4 Hz bandwidth (2) and in 30 Hz bandwidth (4); (3), reference signal. (b) subharmonic signals in 4 Hz bandwidth from two probes; (5), $z = -2.5$ mm, (6), $z = +12.5$ mm. Principal regime, $x = 640$ mm ($R = 628$), $y/\delta = 0.26$.

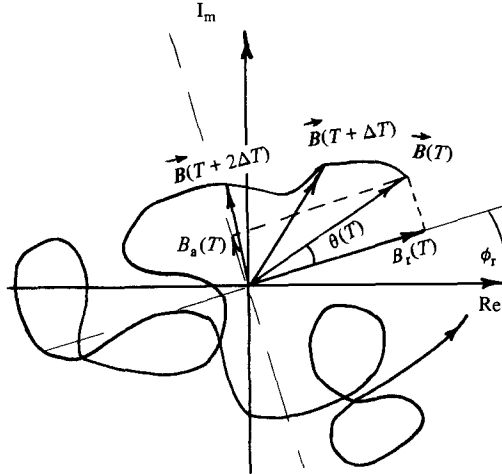


FIGURE 7. Qualitative picture of movement of priming oscillations vector at uncontrolled conditions. $B_r(t)$ = resonant component; $B_a(t)$ = damping component.

resonance) have a definite phase and a non-zero amplitude. In contrast, ‘priming’ fluctuations decay in the case of the orthogonal phase.

‘Priming’ subharmonic oscillations with an amplitude $A(T)$ and a phase $\phi(T)$, slowly changing in the time, can be represented in the form

$$u'_2 = B_2(T) \exp(-i\omega_2 t), \tag{1}$$

where $B_2(T) = A_2(T) \exp[i\phi_2(T)]$ is a complex amplitude vector. Of course, $A_2(T)$ and $\phi_2(T)$ are considered to be slowly changing during a subharmonic period T_2 .

A vector diagram of the evolution of a vector $B_2(T)$ with a (slow) time is represented qualitatively in figure 7. The curved line corresponds to the trajectory of a movement of the end of a vector $B_2(T)$. Three subsequent positions of a vector are also shown.

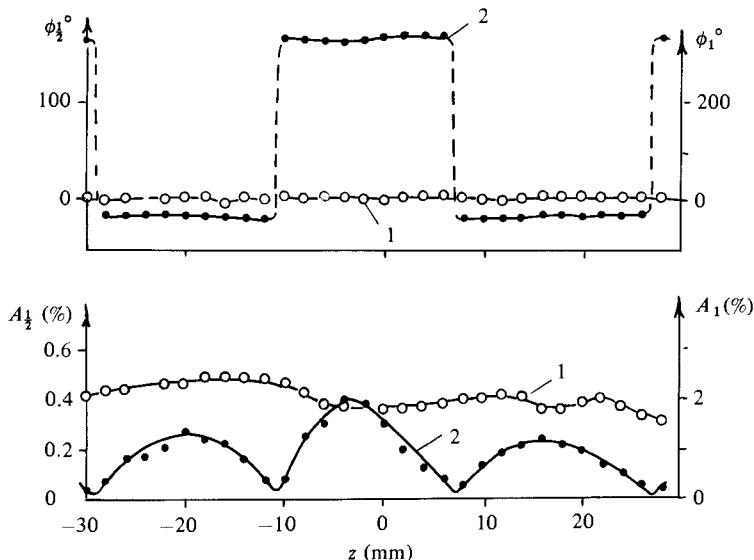


FIGURE 8. z -distributions of amplitudes and phases of fundamental wave (1) and subharmonic (2); $f_1 = 96.4$ Hz ($F_1 = 109 \times 10^{-6}$), $x = 600$ mm ($R = 608$), $y/\delta = 0.26$.

At the arbitrary moment of 'slow' time T , a 'priming' disturbance can be represented as the superposition of components with 'resonant' and 'antiresonant' phases which corresponds to components $B_r(T)$ and $B_a(T)$ in figure 7. In accordance with the aforesaid, only the projection of a randomly oscillating amplitude vector of a priming $B_2(T)$ in the resonance direction, given by the subharmonic phase ϕ_r favourable (resonant) relative to the fundamental wave, is always in the parametric resonance. Depending on the value of this projection, the amplitude and the phase of the resonantly amplified subharmonic change with the time.

A slowness of the change of $B_2(T)$ with time means from the spectral point of view that the given quasi-stationary interpretation of the resonance onset is correct for sufficiently narrow packets of 'priming' fluctuations near frequency f_2 . If a spectrum of 'priming' low-frequency fluctuations is broad, it is more convenient to operate with the concept of the 'spectral width of resonance', which is characterized, for instance, by the width of a packet amplified by means of resonance from a continuous spectrum of 'priming' oscillations. This resonance width Δf_r determines (in time) a characteristic period of beats of the resonantly amplified subharmonic.

3.3. Existence of synchronism

The measurements showed that subharmonic fluctuations were three-dimensional in the region of their rapid amplification. The amplitudes and phases of the fundamental wave and the subharmonic versus the spanwise coordinate z are shown in figure 8 for the regime $f_1 = 96.4$ Hz. The analogous picture for the principal regime of the measurements ($f_1 = 111.4$ Hz) is given in figure 9(a). The synchronous oscilloscope traces of the oscillations with the frequency f_2 (at 4 Hz bandwidth) at points $z = -2.5$ mm and $z = 12.5$ mm are given in figure 6(b).

The 180° jumps of the subharmonic phase in the regions of minima in z -distributions of amplitude are the characteristic feature of the represented data. The observed distributions of amplitudes and phases of the subharmonic correspond to a pair of oblique waves, propagating with angles that are equal to each other but have opposite

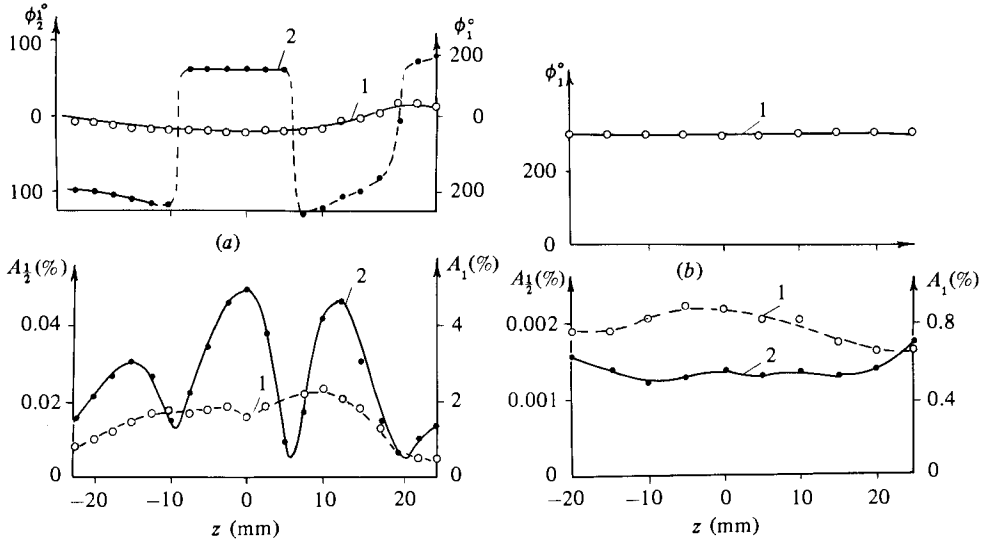


FIGURE 9. z -distributions of amplitudes and phases of fundamental wave (1) and subharmonic (2); principal regime; $y/\delta = 0.26$: (a), $x = 600$ mm ($R = 608$); (b), $x = 300$ mm ($R = 430$).

direction relative to the mean flow. Indeed, the sum of such two waves can be presented in the form

$$B_2^+(T) \exp[i(\alpha_2 x + \beta_2 z - \omega_2 t)] + B_2^-(T) \exp[i(\alpha_2 x - \beta_2 z - \omega_2 t)] \\ = B_2(T) \cos(\beta_2 z) \exp[i(\alpha_2 x - \omega_2 t)] \quad (2)$$

(where $B_2 = B_2^+ + B_2^-$, $B_2^+ = B_2^-$ are the complex amplitudes of oblique waves), which corresponds to the distributions in figures 8 and 9(a) and gives the space beats of the standing-wave type in the direction of the z -axis. The beat period is $\lambda_z = 2\pi/\beta_2$, and the interval between antinodes is $\frac{1}{2}\lambda_z = \pi/\beta_2$.

In the principal regime ($f_1 = 111.4$ Hz) at $x = 600$ mm ($R = 608$) the value β_2 is equal to 0.207 mm^{-1} ; $\beta_2 \delta^* = 0.352$, and at $f_1 = 96.4$ Hz $\beta_2 = 0.168 \text{ mm}^{-1}$, $\beta_2 \delta^* = 0.286$ (here and henceforth $\delta^* = 1.7208(\nu x/u_\infty)^{1/2}$).

It should be mentioned that at the initial section $x = 300$ mm ($Re = 430$) the z -distributions of the amplitude and the phase for the fundamental wave and the z -distribution of the subharmonic amplitude have a rather smooth, quasi-two-dimensional nature, as is seen in figure 9(b). The subharmonic phase does not have a definite value in this section. In the region of subharmonic amplification a dependence of the fundamental wave amplitude on z increases gradually, but the fundamental wave phase is almost constant as before (figures 8, 9a).

The main condition for the existence of a three-wave nonlinear resonance, in particular of the parametric resonant amplification, is the condition of phase synchronism (Raetz 1959; Craik 1971)

$$\omega_1 = \omega_2 + \omega_3, \quad \alpha_1 = \alpha_2 + \alpha_3. \quad (3)$$

In the case of the excitation of a pair of oblique subharmonics $\alpha_2 = \alpha_3 = \alpha_{\frac{1}{2}}$ and $\omega_2 = \omega_3 = \omega_{\frac{1}{2}}$, and conditions (3) in this case reduce to

$$\left. \begin{aligned} \omega_1 &= 2\omega_{\frac{1}{2}}, & \alpha_1 &= 2\alpha_{\frac{1}{2}} \\ \omega_{\frac{1}{2}} &= \frac{1}{2}\omega_1, & \frac{\omega_1}{\alpha_1} &= \frac{\omega_{\frac{1}{2}}}{\alpha_{\frac{1}{2}}} \end{aligned} \right\} \quad (4)$$

or

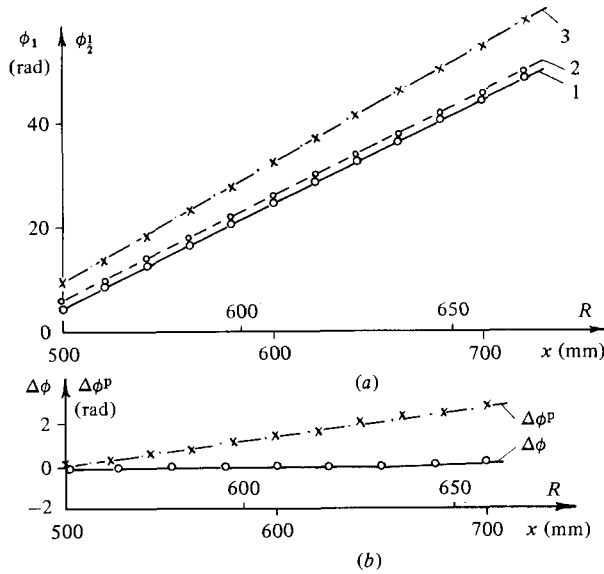


FIGURE 10. Synchronization of phases of fundamental wave (1) and subharmonic (2) at resonance; (3), plane Tollmien–Schlichting wave with frequency $\frac{1}{2}f_1$; $\Delta\phi^p$, difference of phases (3)–(1). Principal regime; $z = -2.5$ mm, $y/\delta = 0.26$.

It is possible to rewrite the last equation in the form

$$|C_1| = \frac{|C_{\frac{1}{2}}|}{\cos \theta_{\frac{1}{2}}},$$

where $C_1, C_{\frac{1}{2}}$ are phase-velocity vectors for a fundamental wave and a subharmonic, $\theta_{\frac{1}{2}}$ is the angle between the vector $C_{\frac{1}{2}}$ (or the subharmonic wavevector $K_{\frac{1}{2}}$) and the vector C_1 (or the mean-flow direction).

The synchronism conditions (4) mean that the speed $V_{x_{\frac{1}{2}}}$ with which it is necessary to move along the x -axis in order that the subharmonic phase should not depend on the time, has to be equal to the corresponding speed V_{x_1} for the fundamental wave. It is easy to show that for this speed

$$V_x = \frac{\omega}{|K| \cos \theta} = \frac{|C|}{\cos \theta} = \frac{\omega}{\alpha},$$

and so the equality $V_{x_{\frac{1}{2}}} = V_{x_1}$ is equivalent to the synchronism conditions (4). In other words, for existence of a synchronism the difference of phases for the fundamental wave ϕ_1 and the subharmonic $\phi_{\frac{1}{2}}$ has to remain constant in the downstream direction if both of them are calculated in parts of the fundamental wave (or the subharmonic) period.

The x -distributions of the phases of the fundamental wave $\phi_1(x)$ and the subharmonic $\phi_{\frac{1}{2}}(x)$ for the principal regime, measured in radians of the fundamental wave period, are presented in figure 10(a). For comparison, the corresponding distribution of the phase $\phi_{\frac{1}{2}}^p(x)$ of the two-dimensional Tollmien–Schlichting wave of frequency $f_{\frac{1}{2}}$ is given, as, instead of oscillations of frequency f_1 , the small-amplitude oscillations of frequency $f_{\frac{1}{2}}$ were excited by the vibrating ribbon. It can be seen that, all dependences are straight lines and correspond to the dimensional wavenumbers $\alpha_1 = 0.204$ mm⁻¹, $\alpha_{\frac{1}{2}} = 0.103$ mm⁻¹, $\alpha_{\frac{1}{2}}^p = 0.113$ mm⁻¹. The corresponding values of the phase differences

| f_1 (Hz) | $F_1 \times 10^6$ | α_1 (mm ⁻¹) | β_1 (mm ⁻¹) | $\frac{\beta_1}{\alpha_1}$ | θ_1 | C_{x_1} (m/s) | $\alpha_1 \delta^*$ | $\beta_1 \delta^*$ | $\frac{C_{x_1}}{U_\infty}$ | V_{x_1} (m/s) | $\frac{V_{x_1}}{U_\infty}$ |
|---------------|-------------------|-----------------------------------|----------------------------------|----------------------------|------------|--------------------|---------------------|--------------------|----------------------------|--------------------|----------------------------|
| 55.7 | 62.0 | 0.103 | 0.207 | 2.01 | 63.6° | 0.674 | 0.175 | 0.352 | 0.073 | 3.40 | 0.37 |

TABLE 1

| f_1 (Hz) | $F_1 \times 10^6$ | α_1^p (mm ⁻¹) | $C_{x_1}^p$ (m/s) | $\alpha_1^p \delta^*$ | $\frac{C_{x_1}^p}{U_\infty}$ | α_1 (mm ⁻¹) | $\alpha_1 \delta^*$ | $C_{x_1} \equiv V_{x_1}$ (m/s) | $\frac{V_{x_1}}{U_\infty}$ |
|---------------|-------------------|-------------------------------------|----------------------|-----------------------|------------------------------|-----------------------------------|---------------------|-----------------------------------|----------------------------|
| 111.4 | 124 | 0.113 | 3.10 | 0.192 | 0.34 | 0.204 | 0.347 | 3.43 | 0.37 |

TABLE 2

$\Delta\phi = \phi_1 - \phi_2$ and $\Delta\phi^p = \phi_1^p - \phi_2^p$, measured in parts of the fundamental wave period, are shown in figure 10(b). The constancy of $\Delta\phi$ and the measured values of α_1 and of α_2 testify to the fulfilment of the synchronism conditions (4) within measurement errors. Analogous results were obtained in the regime with $f_1 = 96.4$ Hz. In particular, $\alpha_2 = 0.085$ mm⁻¹, $\alpha_2 \delta^* = 0.175$ at $x = 600$ mm.

After determining values of α_1 and β_1 for components of $\mathbf{K}_1^+ = (\alpha_1, \beta_1)$, $\mathbf{K}_1^- = (\alpha_1, -\beta_1)$, it is possible to determine phase-velocity vectors and propagation angles of excited subharmonics:

$$C_{x_1}^\pm = \frac{\omega_1}{|\mathbf{K}_1^\pm|^2} \mathbf{K}_1^\pm, \quad \theta_1^\pm = \pm \arctan \frac{\beta_1}{\alpha_1},$$

in particular,

$$C_{x_2}^\pm = \frac{\omega_2 \alpha_2}{\alpha_2^2 + \beta_2^2}.$$

The results of corresponding calculations are brought together in table 1 ($x = 600$ mm, $R = 608$, $\delta^* = 1.70$ mm, $U_\infty = 9.18$ m/s).

For the fundamental wave and the plane Tollmien–Schlichting wave with a subharmonic frequency, the results are given in table 2 (for the principal regime).

Propagation angles for the subharmonics are about 63°–64° in both regimes, and the values of β_2/α_2 are about 2.

It should be mentioned that this value of θ_2 differs somewhat from theoretical ones. Thus calculations by Volodin & Zelman (1978) for the point of the exact (without detuning) realization of the resonance conditions ($R = 636$, $F = 124 \times 10^{-6}$) gave values of wavevector components as $\alpha_2 = 0.19$, $\beta_2 = 0.197$, i.e. $\beta_2/\alpha_2 = 1.04$ and $\theta_2 = 46^\circ$. The calculations was carried out at fixed β_2 , and the propagation angle of the subharmonic changed from $\theta_2 = 50^\circ$ for $R = 549$ up to $\theta_2 = 44^\circ$ for $R = 723$.

In the present experiment, the x -component of the phase velocity C_{x_2}/U_∞ is equal to 0.073 in the principal regime ($F_2 = 62 \times 10^{-6}$), which coincides with the corresponding value for the Tollmien–Schlichting wave with frequency $F = 64 \times 10^{-6}$ ($f = 55$ Hz) having propagation angle $\theta_2 = 66^\circ$ (see Gilyov *et al.* 1981). For plane waves with the same frequencies both in the present experiment and in the experiment by Gilyov *et al.*, phase velocities coincide: $C_{x_2}^p/U_\infty = 0.34$. These comparisons in addition confirm that (in principal regime) the conditions of synchronism occur and they are realized just for waves propagating under angles $\theta_2^\pm \approx 64^\circ$. Their realization can be seen also from tables 1 and 2 as the fact that $V_{x_2} = V_{x_1} = 0.37$ (but $C_{x_2} \neq C_{x_1}$!). It can be noted that as observed in the pictures by Saric, Carter & Reynolds (1981),

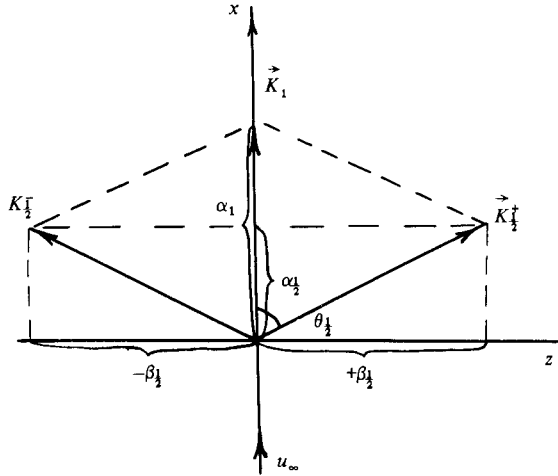


FIGURE 11. Experimentally detected triad of waves. Principal regime. Values of parameters are given in tables 1 and 2.

the ratio $\beta_{1/2}/\alpha_{1/2}$ is approximately equal to 2, which again supports the experimental value of the resonance angle $\theta_{1/2} = 63^\circ\text{--}64^\circ$ (of course in the studied range of parameters). Apparently, the difference of this value from the theoretical one can be explained by a very slow dependence of α on β (see e.g. Gilyov *et al.* 1981, figures 29, 35). At small values of $d\alpha/d\beta$ a small error $\Delta\alpha$ in a calculation of the dependence $\alpha_{1/2} = \alpha_{1/2}(\beta)$ (due to neglecting non-parallelism effects, for instance) can result in a large error $\Delta\beta$ in the determination of the resonance value $\beta_{1/2}$ from the condition $\alpha_{1/2}(\beta) = \frac{1}{2}\alpha_1$, because $\Delta\beta = \Delta\alpha/(d\alpha/d\beta)$.

Hence the analysis of x - and z -distributions of subharmonic amplitudes and phases shows that the excited oscillations with the frequency $f_{1/2} = \frac{1}{2}f_1$ are the pair of oblique waves for which the conditions of the existence of the three-wave resonance, described theoretically by Raetz (1959), Craik (1971) and Volodin & Zelman (1978), are realized. The development of the fundamental wave does not depend on the subharmonic development in an initial region of the amplification of small 'priming' subharmonic fluctuations (figure 2), and the resonance is in fact the parametric resonance (see Volodin & Zelman 1978) whose properties determine the detected features of the behaviour of amplitudes and phases of the fluctuations with frequency $f_{1/2}$. The experimentally detected resonant triad of waves is presented in figure 11 as a vector diagram.

3.4. Amplitude and phase profiles

The normal-to-the-wall distributions of amplitudes and phases of the fundamental wave and the subharmonic at $x = 650$ mm ($R = 633$) for the principal regime are given in figure 12(a). The profiles of the amplitude and the phase are typical ones for Tollmien-Schlichting waves in the region of the second branch of the neutral curve. The amplitude of the subharmonic has one clear maximum approximately in the critical layer $y = y_c$, which is the same for f_1 and $f_{1/2}$, because the synchronism condition is fulfilled (i.e. $\omega_{1/2}/\alpha_{1/2} = V_{x_{1/2}} = V_{x_1} = \omega_1/\alpha_1$). A maximum in the y -profile of the subharmonic is almost absent outside the boundary layer. As a whole the form of the y -profile of the subharmonic amplitude is like the corresponding distributions obtained by Gilyov *et al.* (1981) for linear oblique Tollmien-Schlichting waves. The distribution of the phase of the subharmonic has the characteristic form of a 'dipper'.

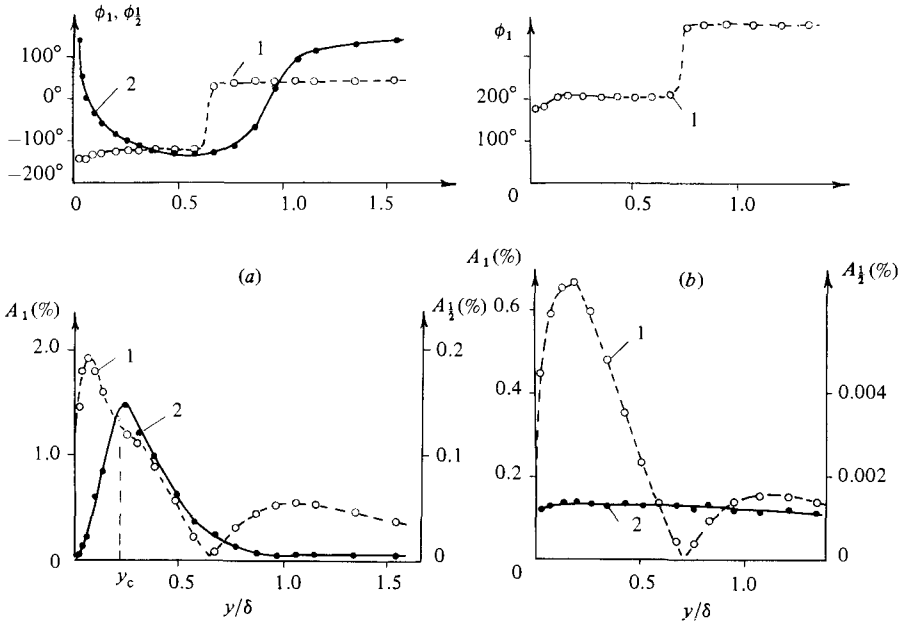


FIGURE 12. Profiles of amplitudes and phases for fundamental wave (1) and subharmonic (2) in the region of resonant amplification (a), $x = 650$ mm ($R = 633$) and in initial point (b), $x = 300$ mm ($R = 430$).

For this distribution a second zone of a strong shear of the phase near the wall is characteristic. This distribution differs from the usual phase profiles of plane Tollmien–Schlichting waves, but again it is like the form of the profile for oblique (three-dimensional) eigenoscillations of a boundary layer, which were studied experimentally by Gilyov *et al.* (1981). In turn Gilyov *et al.* (1981) had mentioned the good correspondence of their experimental y -profiles of disturbances for oblique waves to theoretical profiles given by Craik (1980).

Such y -profiles of amplitudes and phases of oscillations with frequency f_2 are formed as a result of the resonant excitation of the subharmonic out of initial disturbances which have a profile $A_{1/2}(y)$ shown in figure 12(b). As was mentioned, the phase of oscillations does not have a definite value here. Also shown in figure 12(b) are initial distributions of amplitudes and phases of the fundamental wave $A_1(y)$ and $\phi_1(y)$.

Mean-velocity profiles, measured at $x = 300$ – 650 mm corresponded to a Blasius profile to within 1%. A distortion of the mean-flow velocity by disturbances was not observed in this x -range. A deviation of mean-velocity profiles from the Blasius laminar profile had been observed downstream from this range in the region of formation of a ‘bell-like’ form of the fundamental wave profile (see §3.1). A form of mean-velocity profile in this region had been studied by Kachanov *et al.* (1977) (see also Kachanov 1978).

3.5. Growth curves for disturbance amplitudes

The measurements of growth curves for the amplitudes of disturbances were made in the region of the maximum of subharmonic y -profiles at $y/\delta = 0.26$. This coordinate was close to the coordinate of the maximum of the fundamental wave at the beginning of the measurement region (see figure 12).

The growth curves for the amplitudes of the fundamental wave and the subharmonic in the principal regime are presented in figure 13. The amplitude of the fundamental

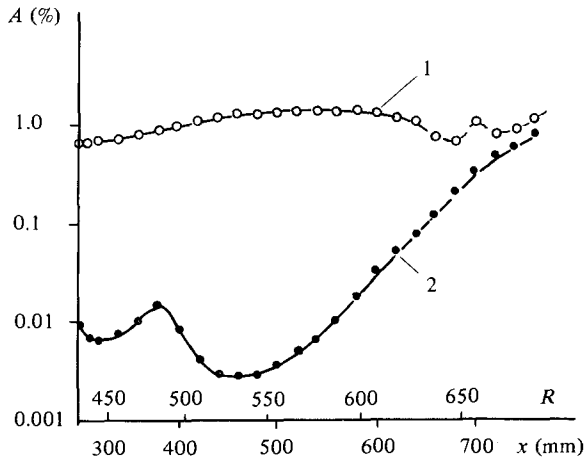


FIGURE 13. Amplification curves for fundamental wave (1) and subharmonic (2).
Principal regime, $y/\delta = 0.26$, $z = -2.5$ mm.

wave grows inside the neutral stability curve and then decays in the region after the second neutral branch. In figure 13 the decay begins a little earlier than in the theory (see figure 23(b)), that is connected with a moving of the maximum in the profile $A_1(y)$ to the wall because of non-parallelism effects (see Kachanov, Kozlov & Levchenko 1975, 1977; Saric & Nahfeh 1975).

The measurements showed that the fluctuations with frequency f_2 at $x \leq 480$ mm ($R \leq 543$) had no definite phase values, i.e. they were not correlated with the fundamental wave and were some background fluctuations with a continuous spectrum. Beginning from $x = 500$ mm ($R = 555$) it is possible to indicate some definite value around which the phase oscillates, which means the appearance of the resonant amplified subharmonic. Beginning from $x = 540$ mm ($R = 577$) the phase of the fluctuations with the frequency f_2 ceases to oscillate and gains a fixed value. It means that here and further the resonantly amplified subharmonic predominates considerably over background fluctuations – a source of a phase noise. On the length $x = 540$ – 700 mm ($R = 577$ – 657) a practically exponential growth of the subharmonic amplitude is observed, the amplification rates being much larger than those in the linear theory.

It should be mentioned that the amplitude of the fundamental wave is almost constant in this region – a neighbourhood of the second branch of the neutral curve (taking into account a movement of the maximum to the wall). Then the subharmonic becomes equal to the fundamental wave in amplitude. Approximately in this place, large deviations of fundamental wave amplification rate from a linear law and a large deformation of a profile $A_1(y)$ are observed, which indicates the onset of the breakdown of the laminar regime (see the end of region II in Kachanov *et al.* 1977). A large low-frequency vibration of the total hot-wire anemometer signal was observed on the oscilloscope screen in this region (see figure 6, trace 1). It should be mentioned here that no indications of breakdown were observed in this region as a subharmonic had been amplified from a time-controlled priming (see §4.4).

3.6. Evolution of fluctuation spectra

The amplitude spectra of velocity fluctuations for different downstream positions, for $y/\delta = 0.26$, at the principal regime are given in figure 14(a). In the initial

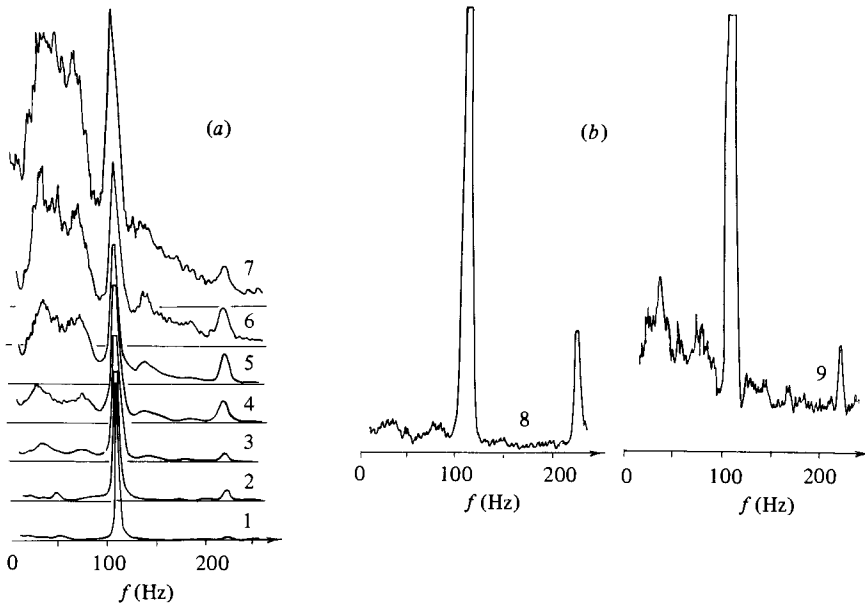


FIGURE 14. (a) x -evolution of amplitude spectra of fluctuations: curves 1, 2, 3, 4, 5, 6, 7 for $x = 300, 480, 600, 640, 680, 720, 760$ mm, $z = -2.5$ mm. (b) z -evolution of amplitude spectra of fluctuations: curves 8, 9 for $z = -2.5, +5.0$ mm; $x = 600$ mm.

spectrum, the fundamental wave with frequency $f_1 = 111.4$ Hz and its second harmonic $f_2 = 2f_1$ are presented mainly. Some rises on the frequencies of 16 and 32 Hz are connected with the vibration background of the facility (see e.g. the vibration spectra in Kachanov 1978). Small peaks on frequencies, divisible by the frequency of 50 Hz, are interference from the electric network.

At $x = 480$ mm ($R = 543$) the spectrum is almost unchanged qualitatively. The appearance of the small third harmonic is observed here.

In the region where a rapid resonant amplification of the subharmonic is observed, the spectra demonstrate a singling out and rapid amplification of a low-frequency oscillation packet having two maxima of frequencies $f^* \approx 34$ Hz and $f^{**} \approx 77$ Hz. As had been mentioned in Kachanov *et al.* (1977) the relation $f^{**} \approx f_1 - f^*$ or what is the same, $\frac{1}{2}(f^* + f^{**}) \approx f_1$ takes place for f^* and f^{**} , i.e. the subharmonic is the centre of the packet. An amplification of the combination modes $nf_1 \pm f^*$, where $n = 1, 2, 3$, is observed too. In this way the gradual filling and smoothing of the spectrum begin when all of these spectral components grow ($x = 720, 760$ mm, $R = 667, 689$).

The process proceeds by the same way as in the experiments of Kachanov *et al.* (1977). The appearance of 'definite low-frequency fluctuations' f^* and f^{**} is as a signal to the beginning of the spectrum filling, which proceeds by the way of an interaction of growing components f^* , f^{**} with the fundamental wave and its harmonics, with the generation of combination modes. It was mentioned in Kachanov *et al.* (1977) that the frequency f^* was quite random, it depended on amplitude and a frequency of the fundamental wave, but the nature of this dependence has not been understood. Rabinovich (1978) had suggested that the modulation instability of the fundamental wave is the reason of the excitation of harmonics of $f_1 \pm f^*$ type. However, this suggestion was scarcely argued.

3.7. Reasons for excitation of incommensurable low-frequency fluctuations

It is necessary to mention the four following important circumstances.

First, although a considerable rise in amplitude spectra in the immediate neighbourhood of the frequency $f_{\frac{1}{2}}$, except the last sections $x = 720, 760$ mm, is not observed (this prevented the detection of the subharmonic early and made it difficult to search for it in the work of Kachanov *et al.* 1977), the central frequency of a low-frequency fluctuation packet is close to $f_{\frac{1}{2}}$, and $\frac{1}{2}(f^* + f^{**}) \approx \frac{1}{2}f_1$ (see §3.6 and figure 14*a*).

Secondly, the analysis of the oscilloscope traces in figures 5 and 6 shows that antinodes in subharmonic oscilloscope traces, both at the analyser bandwidth of $2\Delta f = 4$ Hz and $2\Delta f = 30$ Hz, correspond to the slow time moments when the resonant amplification of random priming fluctuations takes place (see §3.2). The resonant nature of subharmonic amplification at these moments of time is corroborated by the fact that the fluctuation phase in antinodes always has a definite (resonant) value ϕ_r even if the antinode length is equal only to 1–2 periods of the subharmonic.

Thirdly, the main energy of low-frequency oscillations in a filtered range of frequencies from $f_{\frac{1}{2}} - \Delta f$ up to $f_{\frac{1}{2}} + \Delta f$ at $x \geq 500$ mm is contained just in these antinodes, i.e. in resonantly amplified fluctuations being scraps of sinusoids of frequency $f_{\frac{1}{2}}$ with a variable amplitude but with a constant phase (figures 5 and 6).

Fourthly, the whole of the low-frequency fluctuation packet, including f^* and f^{**} , has a small amplitude in the z -region, where the amplitude of the resonant subharmonic is small owing to an interface of a pair of oblique waves of type (2). This fact is demonstrated by the spectra in figure 14(*b*) obtained at $z = -2.5$ mm and $z = +5.0$ mm in the principal regime. The form of low-frequency fluctuation packet is practically unchanged, and so amplitudes of all components are changed proportionally to the subharmonic amplitude.

From the listed observations, it is possible to draw the conclusion that *the parametric resonance leads to the amplification not of a narrow spectral harmonic $f_{\frac{1}{2}}$, but of a rather broad packet of low-frequency fluctuations.*

As has been mentioned in §3.2, it means, from the quasi-stationary point of view, a sporadic beginning of the resonance at the intervals of the slow time, when the phase of a priming subharmonic oscillations is favourable for a resonance which leads to the appearance of antinodes having a fixed resonant phase ϕ_r (or $\phi_r + \pi$, which is the same) on the subharmonic oscilloscope traces. At the same time, such beats of amplitudes and jumps of phases from the point of view of the spectral analysis correspond to the presence of a broad packet in the spectrum, which indicates a rather large spectral width of the resonance and a rather broad spectrum of priming fluctuations.

Thus the excitation of mysterious 'definite low-frequency fluctuations' (see Kachanov *et al.* 1977) takes place owing to the resonant parametric amplification of fluctuations with a frequency $f_{\frac{1}{2}}$ from a continuous spectrum of priming oscillations. The peaks on frequencies f^* and f^{**} in spectra are turned out after the Fourier transformation of fluctuations on large times (i.e. in broad integration limits) because of an amplitude modulation of the subharmonic and its phase jumps.

An estimate of the spectral width of the discovered resonance is of interest. The analysis of the oscilloscope traces on frequency $f_{\frac{1}{2}}$ at $x = 600$ mm ($R = 608$) showed that, in the analyser bandwidth of 4 Hz, the most-probable length of the antinode in the time (a duration of the resonance) makes up $T_{\Delta} \approx 0.2$ s, which corresponds to the width of the spectral window of the analyser ($f_{\Delta} = 1/T_{\Delta} \approx 5$ Hz). In the 30 Hz bandwidth, $T_{\Delta} \approx 0.03$ s and $f_{\Delta} \approx 33$ Hz were obtained, which coincide with the values

for the spectral window too. Thus the observed width of a resonantly amplified packet $\Delta f \gtrsim 30$ Hz. Indeed, the spectra in figure 14 (*a*) indicate the width of a rapidly growing packet of low-frequency oscillations be $\Delta f \sim 50$ Hz. Additional estimates will be obtained in § 4.2 from results of experiments with controlled priming disturbances. So a large width of resonance $\Delta f_r \sim f_{\frac{1}{2}}$ means, in particular, that an appreciable amplification of subharmonic oscillations takes place in the space in distances of $\Delta x \sim \lambda_{\frac{1}{2}} = 2\pi/\alpha_{\frac{1}{2}}$. Indeed a characteristic length of the resonantly amplified packet in the space is $\Delta x \sim C_{\frac{1}{2}}/f_{\frac{1}{2}} \sim C_{\frac{1}{2}}/\Delta f_r = \lambda_{\frac{1}{2}}$. Since the amplification is convective (drifting), a packet length defines the distance where the resonance has time to manifest itself, and after that a change of phase of priming oscillations to an unfavourable value at an initial section can no longer influence the result of the amplification.

The results of the measurements show that this feature is present. So in the principal regime $\lambda_{\frac{1}{2}} = 61$ mm. The intensity of resonantly amplified fluctuations grows by a factor of approximately 4.5 in this distance (see figures 13 and 23*a*). It is to be noted too that in the introduction of controlled priming disturbances (§ 4) the resonance has time to stretch a trajectory on the vector diagram at 300 mm, i.e. at a distance of only 50 mm from a vibrating ribbon (see § 4.1, figure 16).

4. Resonant amplification of a controlled subharmonic priming oscillation

4.1. Analysis of oscilloscope traces of resonantly amplified fluctuations

In order to study the process of the parametric resonant excitation of the subharmonic in detail, the experiments in the principal regime were repeated with the introduction of controlled small disturbances of frequency $f' = f_{\frac{1}{2}} + \Delta f$ into a boundary layer. The frequency detuning Δf was changed in the range of ± 30 Hz. These disturbances, introduced (as in the work of Saric & Reynolds 1980) by the same vibrating ribbon and simultaneously with a fundamental wave $f_1 = 111.4$ Hz ($E_1 = 124 \times 10^{-6}$), played the role of a controlled deterministic priming for the subsequent parametric amplification.

The phase of such a priming disturbance relative to the fundamental wave (or to reference signal) of frequency f_1 was slowly changed ('drifted') linearly with a time, $\psi = -\Delta\omega t$. Indeed, oscillations of frequency $f' = f_{\frac{1}{2}} + \Delta f$ can be represented as oscillations of frequency $f_{\frac{1}{2}}$ but with phase depending on the time:

$$u'(t) = A_0 \exp \{i[\alpha x - (\omega_{\frac{1}{2}} + \Delta\omega)t]\} = A_0 \exp \{i[\alpha x - \omega_{\frac{1}{2}}t + \psi(t)]\}. \quad (5)$$

The oscilloscope traces, corresponding to 7 moments of the slow time, are shown in figure 15 (*a*). They demonstrate a time displacement of the phase of a subharmonic priming, containing in the ribbon signal, and the subharmonic from a flow in the initial section ($x = 300$ mm) relative to the reference signal. The dependences of subharmonic amplitudes and phases on a slow time (measured in the periods of $T_{\frac{1}{2}}$), obtained by processing of such oscilloscope traces, are presented in figure 15 (*c*).

Amplitudes and phases of the subharmonic oscillations must undergo complex changes downstream in accordance with the parametric-resonance property to amplify only the priming oscillations having a definite phase ϕ_r or $\phi_r + \pi$ (see § 3.2). Namely, with an initial disturbance of a type (5) in the case $\Delta\omega \ll \omega_{\frac{1}{2}}$, the resonance must appear periodically in time with a period $T_{\Delta} = (2\Delta f)^{-1}$ since the phase $\psi(t) = -\Delta\omega t$, changing in time, takes periodically the resonant values $-\Delta\omega t = \phi_r$ (or $-\Delta\omega t = \phi_r + \pi$).

When there is linear growth of the phase with time, the amplitude of periodically

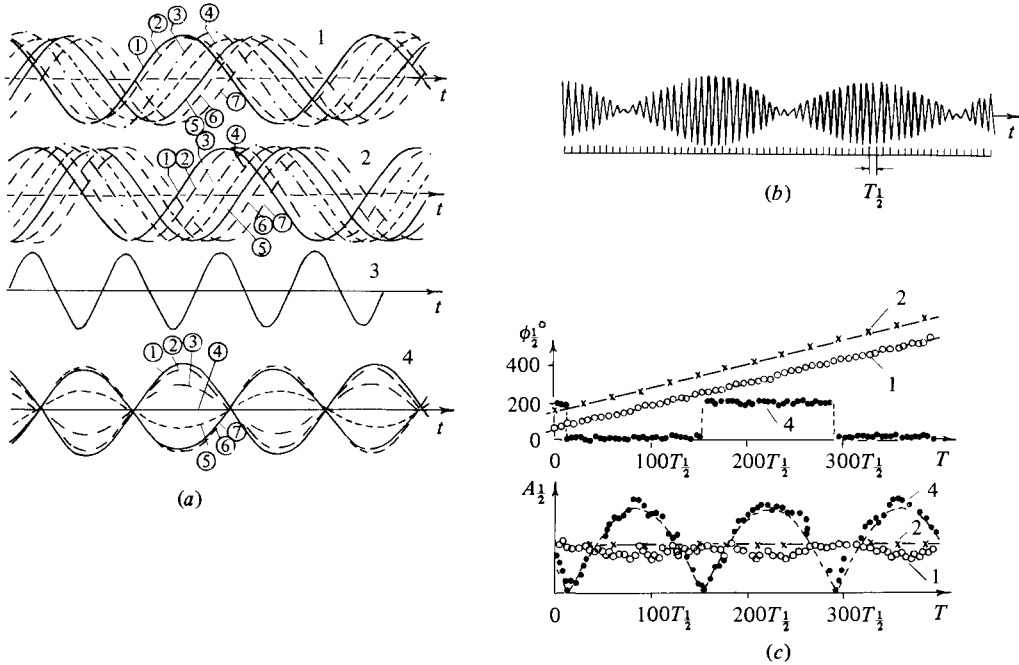


FIGURE 15. Behaviour of amplitudes and phases of fluctuations at controlled conditions. Principal regime. $y/\delta = 0.26$. $z = -2.5$ mm. 1, 4, subharmonic, $x = 300, 650$ mm; 2, priming oscillation; 3, reference signal. (a) oscilloscope trace of subharmonic in 7 moments of slow time; (b) oscilloscope trace of subharmonic in unified timescale; (c) variation of amplitudes and phases on slow time.

amplified oscillations of frequency $f_{\frac{1}{2}}$ must be changed with the time according to law of $|\cos(\Delta\omega t)|$ with periodical jumps of the phase on 180° , because an initial disturbance with any intermediate value of the phase can be expanded into resonant and antiresonant components. Just such a behaviour of the amplitude and the phase of the subharmonic was detected in the region of its amplification ($x \gtrsim 500$ mm, $R \gtrsim 555$). The oscilloscope traces of the subharmonic (in the bandwidth of 4 Hz) in a unified timescale are given in figure 15(b). The beats, meaning the periodic appearance of the resonance at instants when a drifting phase of priming fluctuations (curves 2) gains a resonance value, are well seen. This phenomenon is illustrated in figure 15(a) by the behaviour of the fluctuation amplitude and phase in an expanded scale of the fast time for 7 instants of the slow time (curves 4). A change of the subharmonic amplitude with the time, as expected, is well approximated by the curve $|A_{\max} \cos(\Delta\omega t)|$, marked by the dashed line in figure 15(c).

A vector diagram for priming subharmonic oscillations given to the vibrating ribbon (see (5)) is shown in figure 16(a). It is very close to the diagram for fluctuations of frequency $f_{\frac{1}{2}}$ at $x = 300$ mm, shown in figure 16(b) (see also figure 15(c)). In figure 16(a) there is a uniform slow rotation of a vector $B_{\frac{1}{2}}$, which has a constant modulus, around the origin of coordinates with an angular velocity $\Delta\omega \ll \omega_{\frac{1}{2}}$. It differs from the case of non-controlled priming oscillations, represented qualitatively in figure 7. A resonant amplification of a vector component, having the phase ϕ_r (or $\phi_r + \pi$), from the point of view of a vector diagram, leads in the end to the situation represented in figure 16(c), which corresponds to a predominance of oscillations with resonant phase (see figure 15).

Represented in figure 17(a) oscilloscope traces take place in an intermediate case,

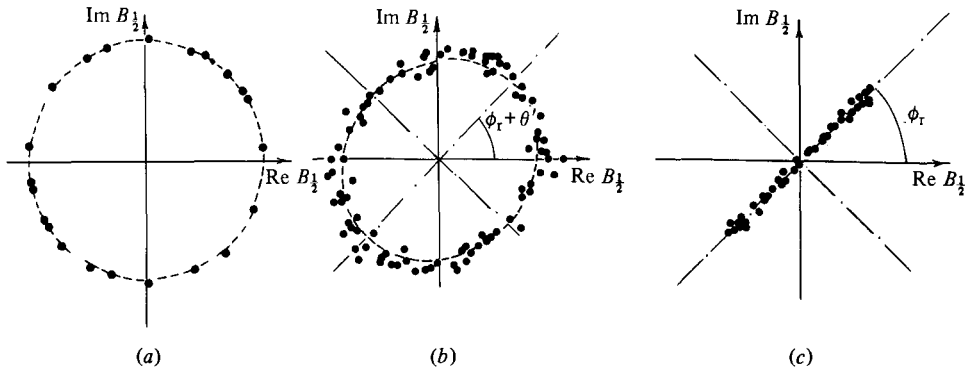


FIGURE 16. Vector diagrams of subharmonic oscillations at controlled conditions. Principal regime. $y/\delta = 0.26$, $z = -2.5$ mm. (a) priming oscillations fed on ribbon; (b) oscillations at $x = 300$ mm; (c) oscillations at $x = 650$ mm.

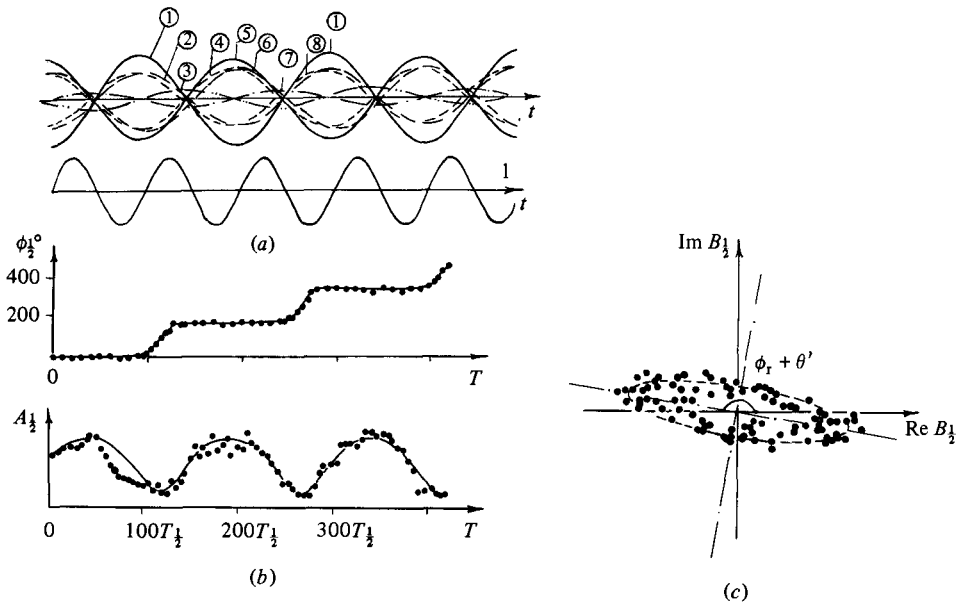


FIGURE 17. Behaviour of amplitudes and phases of subharmonics with slow time. Principal regime. $x = 450$ mm. $y/\delta = 0.26$. $z = -2.5$ mm. (a) oscilloscope traces in 8 moments of slow time: 1, reference signal. (b) dependences of amplitudes and phases on time. (c) vector diagram.

as a parametric interaction of the fundamental wave with the subharmonic fluctuations just began to amplify the oscillations component with phases ϕ_r and $\phi_r + \pi$. The curves correspond to subharmonic oscillations obtained from the hot-wire anemometer probe for 8 moments of the slow time at $x = 450$ mm. The curve 1 is the reference signal. The corresponding dependences of $A_{1/2}$ and $\phi_{1/2}^0$ on the slow time T are shown in figure 17(b). Such oscillations correspond to the rotation of the subharmonic-fluctuation vector $B_{1/2}(T) = A_{1/2} \exp(i\phi_{1/2}^0)$ in the vector diagram along a trajectory of elliptic type (figure 17c).

It is not difficult to show that at $\Delta\omega \ll \omega_{1/2}$ a superposition of boundary-layer eigenoscillations of type (5) with the resonantly amplified pair of oblique subharmonics, which is shifted in phase by an angle $\theta(x)$, gives the oscillations, whose

complex amplitude vector $B_{\frac{1}{2}}(T)$ describes a trajectory in the form of an ellipse on the vector diagram. A phase shift $\theta(x)$ means a difference in phase velocities plane and three-dimensional waves and results in space beats when their amplitudes are approximately equal. The dependence of the phase $\phi_{\frac{1}{2}}$ and the amplitude $A_{\frac{1}{2}}$ of the summed vector $B_{\frac{1}{2}}$ on (slow) time is described by the formulae

$$\phi_{\frac{1}{2}}(T) = \arctan \left\{ \frac{\tan(\Delta\omega T)}{D^{\frac{1}{2}} + (I - D - 1)^{\frac{1}{2}} \tan(\Delta\omega T)} \right\}, \quad (6)$$

$$A_{\frac{1}{2}}(T) = \{a^2 \cos^2[\phi_{\frac{1}{2}}(T) - \theta'(x)] + b^2 \sin^2[\phi_{\frac{1}{2}}(T) - \theta'(x)]\}^{\frac{1}{2}}. \quad (7)$$

The semiaxes of the ellipse are $a = (-A/\lambda_2 D)^{\frac{1}{2}}$, $b = (-A/\lambda_1 D)^{\frac{1}{2}}$. Here I , D and A are invariants of the second order curve, describing the trajectory of the vector $B_{\frac{1}{2}}(T)$; λ_1 , λ_2 are roots of the characteristic equation $\lambda^2 - I\lambda + D = 0$ (see e.g. Korn & Korn 1961). In the formulae (6) and (7) the phase $\phi_{\frac{1}{2}}$ is counted from the resonance phase ϕ_r , and $\theta'(x)$ is the angle of the inclination of the ellipse's principal axis to the line $\phi = \phi_r$. In the space points, where $\theta(x) = 0$, $\theta'(x)$ is also equal to zero. In this case the formula (6) is greatly simplified:

$$\phi_{\frac{1}{2}}(T) = \arctan \frac{\tan(\Delta\omega T)}{\gamma}, \quad (8)$$

where

$$\gamma = \frac{a}{b} = \frac{B_{\frac{1}{2}}^P \exp\left(\int_{x_0}^x \alpha_{iP} dx\right) + B_{\frac{1}{2}}^T \exp\left[\int_{x_0}^x (S - \alpha_{iT}) dx\right]}{B_{\frac{1}{2}}^P \exp\left(\int_{x_0}^x \alpha_{iP} dx\right)}.$$

Here S is an amplification rate of subharmonics at the parametric resonance, which is proportional to an amplitude of the fundamental wave; α_{iP} and α_{iT} are amplification rates of a plane subharmonic and a three-dimensional one in the absence of a resonance, which are determined from linear stability theory; x_0 is the coordinate of the origin of the resonant amplification. $B_{\frac{1}{2}}^P$ and $B_{\frac{1}{2}}^T$ are initial amplitudes of plane and three-dimensional waves having frequency $f_{\frac{1}{2}}$.

It is to be noted that at $x = x_0$ (i.e. before the start of the amplification) $\gamma = (B_{\frac{1}{2}}^P + B_{\frac{1}{2}}^T)/B_{\frac{1}{2}}^P$. It corresponds at $B_{\frac{1}{2}}^T \ll B_{\frac{1}{2}}^P$ to circular motions of a vector of initial (priming) oscillations and coincides with the situation shown in figure 16(a). In contrast, $\delta\gamma \gg 1$ and $\theta' \rightarrow 0$ at very large x or S , i.e. under these conditions a trajectory of vector $B_{\frac{1}{2}}(T)$ approaches a straight line coinciding with the line $\phi = \phi_r$, which corresponds to the situation of figure 16(c). The dependence of the subharmonic amplitude and phase on the time, given by the formulae (6) and (7), correlates well with the experimental points in figure 17(b) (solid line). Here the coefficients a and b in (6) and (7) were determined as semiaxis lengths of the ellipse in figure 17(c).

The resonance is seen to occur already at the 'initial' section $x = 300$ mm, at a distance of 50 mm from the vibrating ribbon. It leads to formation of an ellipse in figure 16(b) with semiaxis ratio $\gamma = 1.2$ (dashed line). γ is equal to 2.78 at $x = 400$ mm, and at $x = 450$ mm the resonance stretches a trajectory of $B_{\frac{1}{2}}$ to the ellipse with $\gamma = 4.58$ (see figure 17c).

The value of $\phi_r = \phi_{\frac{1}{2}} - \phi_1$ does not depend practically on x and z in the region of parametric amplification, and it is changed only with y because the forms of the $\phi_1(y)$ and $\phi_{\frac{1}{2}}(y)$ profiles differ (figure 12, 22). Averaged from a large number

of measurements the value of ϕ_r at $y/\delta = 0.26$ is equal to $81^\circ \pm 7^\circ$ of the subharmonic period, both in the case of amplification of priming oscillations and at the controlled priming. The value ϕ_r is equal to $89^\circ \pm 7^\circ$ in the critical layer ($y/\delta = 0.22$ at $R = 633$), i.e. $\phi_r \approx \frac{1}{2}\pi$ within the error. Values of ϕ_r correspond here to the phase shift between crests of the fundamental wave and the subharmonic. The value $\phi_r \approx \frac{1}{2}\pi$ manifests itself on observation of signals on the oscilloscope screen as a vibration of troughs of the fundamental wave in the summed signal in the region of large amplitudes of the resonantly amplified subharmonic, while the crests of the fundamental wave are practically fixed (the oscillation with subharmonic frequency crosses the zero value here). This peculiarity is seen well in figure 6, line 1. The angle between the principal axis of the ellipse and the abscissa axis in figure 16(c) is not equal to 90° , because the phase was counted not from the fundamental wave but from the reference signal. A scatter of points in figures 15(c), 16 and 17 is connected with no very large predominance of the subharmonic fluctuations, amplified from the imposed priming (figure 16a), over background random fluctuations of frequency $f_{\frac{1}{2}}$ (compare $A_{\frac{1}{2}}(x)$ in figure 13 with that in figure 23a).

Using the method described by Volodin & Zelman (1978), Zelman & Maslennikova (1982) carried out numerical calculations of subharmonic and fundamental-wave amplification. In particular they have obtained data for different initial phase shifts $\Delta\phi = \phi_{\frac{1}{2}} - \phi_1$. The results of the calculations showed that when an initial phase of a subharmonic is orthogonal to its resonance value, i.e. $\Delta\phi = \phi_r + \frac{1}{2}\pi$, the subharmonic not only fails to grow but it also damps with the same rate approximately as at $\Delta\phi = \phi_r$. Other things being equal, it lags behind the subharmonic, having $\Delta\phi = \phi_r$, an order of magnitude or more in amplitude, and then it begins to grow. The amplification is connected with a detuning, taking place at a downstream change of Reynolds number. The detuning results in a change of $\Delta\phi$ and appearance of an oscillation component with the resonant phase $\phi_{\frac{1}{2}} - \phi_1 = \phi_r$ which begins to grow. However, subharmonic amplification rates, at the initial value $\Delta\phi = \phi_r + \frac{1}{2}\pi$, cannot of course exceed their maximum value, at $\Delta\phi = \phi_r$, and therefore the amplitude of the subharmonic at the initial value $\Delta\phi = \phi_r + \frac{1}{2}\pi$ remains always an order of magnitude or more less than its amplitude at initial value of $\Delta\phi = \phi_r$.

4.2. Spectral width of resonance

An evolution of trajectories on the vector diagram described in §4.1 (figure 16, 17c) means, from the spectral point of view (a large-time analysis), an evolution of spectra shown qualitatively in figure 18. As a result of the resonance, a priming disturbance with a frequency $f' = f_{\frac{1}{2}} - \Delta f$, having a constant amplitude and phase (figures 15, 16a, amplitude spectra in figure (18a)), turns into an oscillation of frequency $f_{\frac{1}{2}}$, with amplitude oscillations and phase jumps according to the law of $\cos(\Delta\omega t)$ (figures 15, 16c), having an amplitude spectrum in the form of two components with frequencies $f_{\frac{1}{2}} - \Delta f$ and $f_{\frac{1}{2}} + \Delta f$, whose amplitude and phase do not depend on the time (figure 18c). The spectrum represented in figure 18(b) corresponds to an intermediate state when the form of the trajectory of a vector $B_{\frac{1}{2}}(T)$ (figure 17) is characterized by an ellipse.

Thus it can be said that the parametric subharmonic resonance leads to the amplification of the pair of spectral components with frequencies $f'_{\frac{1}{2}} = f_{\frac{1}{2}} \pm \Delta f$ in the case of detuning $\Delta f \neq 0$. As represented in figure 19, the amplitude spectra are a direct experimental corroboration of this conclusion, which has been obtained essentially from an analysis of fluctuation oscilloscope traces (§4.1). The spectra were obtained at a fixed position of the probe at $x = 650$ mm ($R = 633$) for different values

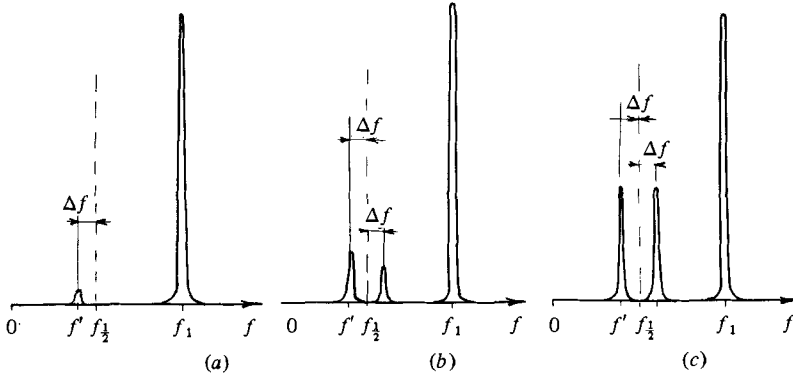


FIGURE 18. Qualitative evolution of spectrum at parametric resonant excitation of controlled subharmonic priming; Δf = frequency detuning.

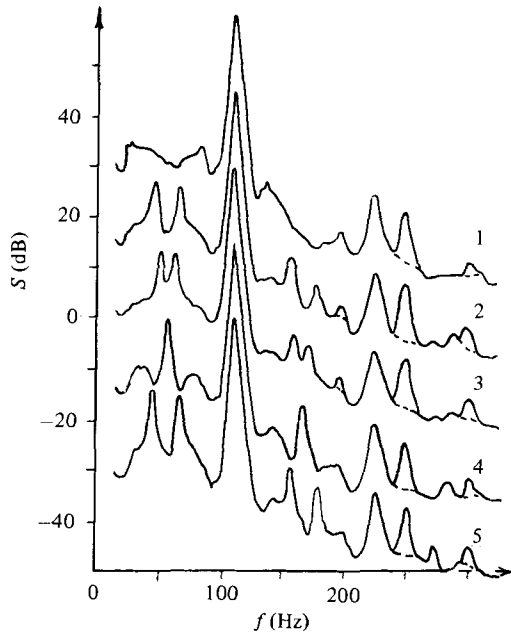


FIGURE 19. Spectra at different frequency detunings between the priming oscillation and $\frac{1}{2}f_1$; 1, 2, 3, 4, 5 correspond to $f = -30, -10, -5, 0, +10$ Hz. Principal regime. $x = 650$ mm ($R = 633$), $y/\delta = 0.26$, $z = -2.5$ mm.

of detuning Δf between frequencies of priming oscillations and the subharmonic. Each subsequent spectrum is moved relatively to the previous one downwards by 15 dB.

The spectra given in figure 19 demonstrate a large spectral width of the resonance, i.e. a resonant excitation of disturbances with frequencies $f' = f_1/2 \pm \Delta f$ takes place even at large detunings. A resonant amplification of priming oscillations is observed at detuning $\Delta f = -30$ Hz (spectrum 1 in figure 19). It is possible to make an estimate of the spectral width of the resonance Δf_r from spectra in figure 19, defining Δf_r as $\Delta f_r = 2\Delta f$, where Δf leads to decrease in amplitude of resonantly amplified fluctuations in two times in comparison with their amplitudes at $f = 0$, and assuming a linearity of the amplitude–frequency characteristic of a vibrating ribbon in the

frequency range $f_{\frac{1}{2}} \pm 30$ Hz (the eigenfrequency of the ribbon $f_0 \approx 120$ Hz). The amplitude of excited fluctuations was found to be the average twice below a corresponding value at $\Delta f = 0$ when the detuning $\Delta f = \pm 20$ Hz. It gives an estimate $\Delta f_r = 2\Delta f \approx 40$ Hz, which corresponds well to the estimate $\Delta f_r \approx 50$ Hz obtained for the case of a natural (non-controlled) subharmonic priming (§3.7).

It is to be noted that spectra on introduction of priming oscillations with frequencies $f_{\frac{1}{2}} + \Delta f$ and $f_{\frac{1}{2}} - \Delta f$ are similar (at least for small Δf) and differ only by amplitudes of excited oscillations, which is explained apparently by a slightly greater sensitivity of the ribbon to frequency $f_{\frac{1}{2}} + \Delta f$ than to $f_{\frac{1}{2}} - \Delta f$ at a constant level of voltage on the output of the generator of priming oscillations.

It is noteworthy that spectra in figure 19 are superpositions of a relatively constant background, of resonantly amplified non-controlled disturbances, and discrete components, amplified from a controlled priming and depending on detuning Δf . Special measurements of the oscillations intensity at different frequencies, at a smooth change of detuning Δf with time, confirmed this conclusion. Deviations of the amplitude from a constant value were observed only in the cases as the fixed frequency window of an analyser at some Δf had coincided with $f' = f_{\frac{1}{2}} + \Delta f$ or other discrete harmonics. This result seems to be quite natural and demonstrates the linearity of parametric resonance in the sense that a controlled priming resonates irrespective of non-controlled background priming oscillations.

4.3. Existence of synchronism at excitation of controlled priming oscillations

The study of x -, y - and z -distributions of amplitudes and phases of subharmonic oscillations has been carried out at detuning Δf of frequencies of priming oscillations f' and subharmonic $f_{\frac{1}{2}}$ being equal to 0.25–0.05 Hz, which means $f' \approx f_{\frac{1}{2}}$ practically. However, the introduction of slight detuning was more convenient than the excitation of oscillations with the frequency $f' = f_{\frac{1}{2}}$ coherent to the fundamental wave. This is connected with the presence, in the first case, of slow quasi-stationary beats of a subharmonic amplitude with a period $T_{\Lambda} \approx 2$ –10 s (i.e. the periodical appearance and disappearance of the resonance). In particular, a detuning permitted separation of harmonics in a spectrum which appeared, because of the resonance, from other oscillations (see §4.5). The oscillation amplitude, corresponding to the resonance, was determined as $A_{\frac{1}{2}}(T = T_0)$, where T_0 is a slow time instant where the subharmonic amplitude was maximum, i.e. $A_{\frac{1}{2}}(T_0) = \max \{A_{\frac{1}{2}}(T)\}$.

The measurements showed that all properties of amplitude and phase distributions for subharmonic oscillations, amplified from the controlled priming, coincide practically with corresponding properties for the case of non-controlled priming fluctuations (see §3).

The distributions $A_{\frac{1}{2}}(z)$ and $\phi_{\frac{1}{2}}(z)$ at $x = 600$ mm ($R = 608$) for the controlled case are represented in figure 20(a). Also given in this figure are the corresponding distributions for the fundamental wave. Like the case of non-controlled priming oscillations, space oscillations of the amplitude of the subharmonic and its phase jumps take place. These indicate an amplification of a pair of three-dimensional waves, symmetrical relative to the flow axis (see §3.3). The synchronous oscilloscope traces in figure 20(b) demonstrate oscillations when the frequency $f_{\frac{1}{2}}$ is in antiphase at the points $z = -15.0$ mm, -2.5 mm, and 12.5 mm. In this case the spanwise components of the wavevectors $K_{\frac{1}{2}}^+$ and $K_{\frac{1}{2}}^-$ have the value $\beta_{\frac{1}{2}} = 0.195$ mm⁻¹, $\beta_{\frac{1}{2}}^* = 0.332$. This coincides with the case of the non-controlled priming (see table 1) within the error of determination of $\beta_{\frac{1}{2}}$ ($\Delta\beta_{\frac{1}{2}} \approx 0.02$ mm⁻¹).

It is to be noted here that initial priming disturbances, not only in the controlled

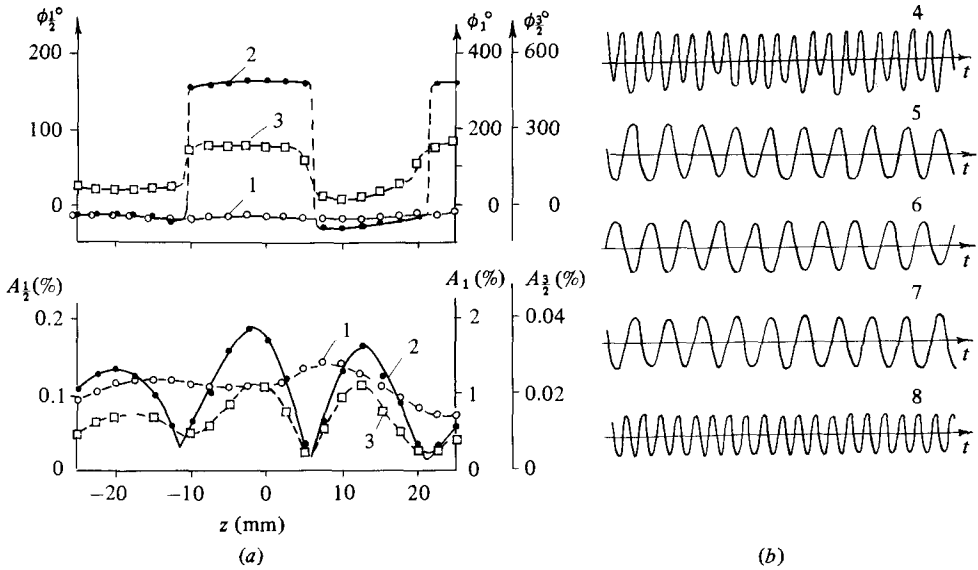


FIGURE 20. z -distributions of amplitudes and phases of fluctuations (a) and oscilloscope traces (b) at controlled conditions. 1, 2, 3, for $f_1, \frac{1}{2}f_1, \frac{3}{2}f_1$; 4, for summary fluctuations ($z = -2.5$ mm); 5, 6, 7, for $\frac{1}{2}f_1$ in 4 Hz bandwidth: $z = -15, -2.5, +12.5$ mm; 8, reference signal. Principal regime. $x = 600$ mm ($R = 608$), $y/\delta = 0.26$.

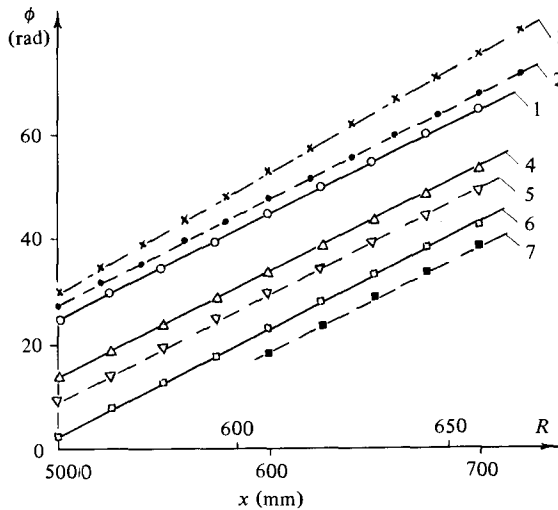


FIGURE 21. Downstream growth of phases of waves at controlled conditions. 1, 2, 3, 4, 5, 6, 7, for $f_1, \frac{1}{2}f_1, \frac{1}{2}f_1^p, 2f_1, 3f_1, \frac{3}{2}f_1, \frac{5}{2}f_1$. Principal regime. $z = -2.5$, $y/\delta = 0.26$.

case but also apparently with non-controlled priming, are initiated, in the main, by the vibrating ribbon, which 'makes a noise' (slowly turbulates a flow) in a broad range of frequencies. In both cases, although an initial spectrum relative to β consists mainly of harmonics with $\beta \approx 0$ (plane waves), it contains also a broad β -spectrum because of the finite length of the ribbon. The parametric resonance leads to emergence from this wave spectrum of the pair of oblique waves $\beta = \pm \beta_{1/2}$ in both cases.

The existence of synchronism (conditions (4)) is demonstrated by disturbance phase distributions, represented in figure 21 (see also §3.3). Wavenumbers determined from

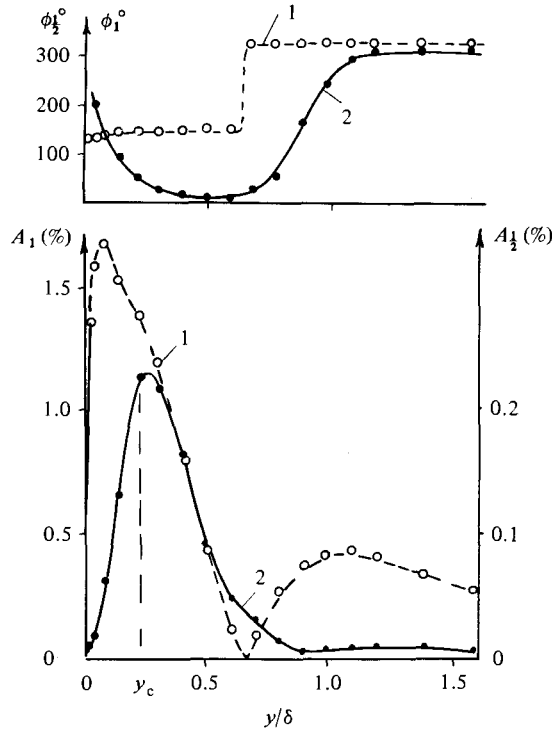


FIGURE 22. y -profiles of amplitudes and phases for fundamental wave (1) and subharmonic (2) at controlled conditions. Principal regime. $x = 600$ mm ($R = 608$), $z = -2.5$ mm.

these distributions have values $\alpha_2 = 0.101$ mm $^{-1}$, $\alpha_2 \delta^* = 0.172$ (at $x = 600$ mm), which gives $\beta_{1/2}/\alpha_2 = 1.93$ and subharmonic propagation angles

$$\theta_{\frac{1}{2}}^{\pm} = \pm \arctan(\beta_{1/2}/\alpha_2) = 62.7^{\circ}.$$

It is evident that the values of α_2 , $\beta_{1/2}$, $\theta_{1/2}$ coincide with good accuracy with corresponding ones for the parametric resonance with a natural random priming (see table 1) and satisfy the synchronism conditions.

Special oscilloscope measurements at the 30 Hz bandwidth of the analyser showed that, within measurement error, a resonant phase-shift value $\phi_r = \phi_{1/2} - \phi_1$ does not depend on the value of frequency detuning Δf of priming oscillations in the detuning range -30 Hz $\leq \Delta f \leq +30$ Hz. They indicate the presence of the phase synchronism even at large detunings. This is possible because of an amplification of a pair of harmonics symmetrical relative to $f_{1/2}$. The phase of each of these harmonics is changed in time, but their superposition gives oscillations of frequency $f_{1/2}$, with amplitude beats and fixed phase (with 180° jumps).

4.4. Profiles and growth curves of fluctuations

Profiles in y of amplitudes and phases of the fundamental wave and the subharmonic, amplified from a controlled priming, are given in figure 22 for $x = 600$ mm (the origins of the phases are arbitrary). It is seen that, as in the case of non-controlled priming, the maximum of the subharmonic is in the region of the critical layer and the phase distribution has a characteristic form of a 'dipper'. The distributions of $A_{1/2}(y)$ and $\phi_{1/2}(y)$ coincide with those in figure 11 in all features.

The growth curves for the fundamental wave and subharmonic are represented in

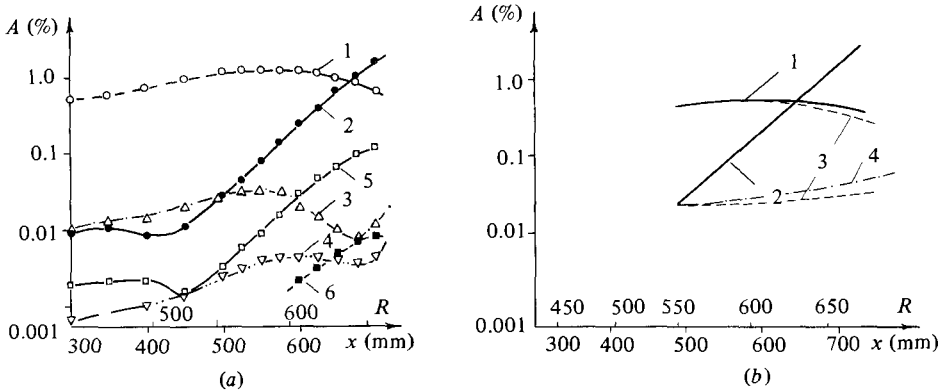


FIGURE 23. Amplification curves. (a) the experiment at controlled conditions; 1, 2, 3, 4, 5, 6, for f_1 , $\frac{1}{2}f_1$, $2f_1$, $3f_1$, $\frac{3}{2}f_1$, $\frac{5}{2}f_1$. Principal regime, $y/\delta = 0.26$, $z = -2.5$ mm. (b) the theoretical calculations by Zelman & Maslennikova. 1, 2, for f_1 (plane wave), $\frac{1}{2}f_1$ (oblique waves) at the resonant interaction; 3, for f_1 (plane wave), $\frac{1}{2}f_1$ (oblique wave) at the linear development; 4, for $\frac{1}{2}f_1$ (plane linear wave). $F = 124 \times 10^{-6}$, points of maxima in y -profiles of wave amplitudes were used.

figure 23(a). As in the case of natural priming (figure 13), a region of an almost exponential amplification of the subharmonic is observed where the fundamental wave amplitude is constant. However, the amplification itself becomes noticeable early, which is connected with an increased initial amplitude of the priming (see §4.2 and the spectra in figure 19). The resonant amplification rate of the subharmonic in this case and in the case of a non-controlled priming (figure 13a) are in good correspondence with each other.

In the controlled case at $x \approx 300$ –350 mm ($R \approx 430$ –464) the subharmonic phase drifts almost uniformly with $\Delta f \approx 0.25$ –0.05 Hz, which indicates a slow manifestation of a resonance (see §3.1). Then, at $x \approx 400$ –450 mm, oscillations of amplitude and phase, corresponding to an elliptical trajectory in figure 17, are observed. Finally, at $x > 450$ mm, a fixed value of the subharmonic phase with 180° jumps and amplitude oscillations, corresponding to predominance of resonantly amplified subharmonic oscillations (see §4.1), are observed.

An amazing property of the fundamental wave in this case should be mentioned here. Its amplitude remains almost independent of the time even at $x = 700$ mm, where the periodically appearing resonance leads to modulation of the amplified subharmonic from a near-zero value up to $A_{\frac{1}{2}} = 2.4A_1$! This points to a periodic transfer of energy from the mean flow to the subharmonic by means of the resonant interaction.

Results of the previously mentioned calculations of Zelman & Maslennikova (1982), carried out for conditions close to those of the present experiments, are represented in figure 23(b). They agree qualitatively with the experiment. Both in the theory and in the experiment in this case, at almost constant fundamental wave amplitude $A_1(x)$ in the region $R = 550$ –650, the subharmonic growth proceeds by the usual exponential law instead of a double-exponential law (see Volodin & Zelman 1978). The experimental amplification rates of subharmonics in this region reach the theoretical values at rather larger amplitudes of the fundamental wave. Apparently, the difference is connected with the extremely large values of the fundamental wave amplitudes in the experiment ($A_1 \sim 1\%$) needed for use in a slow-nonlinear theory, and with a difference in conditions of the experiment and the theoretical model. In

particular, only a few periods of the subharmonic and some non-uniformity of fundamental wave amplitude in the direction of the z -axis are observed in the experiment, while an idealized case of a z -periodic subharmonic and a strictly plane fundamental wave are considered in the theory.

4.5. Behaviour of higher harmonics

As was mentioned in §3.1, oscillations with frequencies $f_2 = 2f_1$ and $f_3 = 3f_1$ had been present in the flow besides the fundamental wave and low-frequency fluctuations. Growth curves for amplitudes of these harmonics are represented in figure 23(a) and their phases, measured in radians of the fundamental wave period, are given in figure 21. The conditions $\omega_1/\alpha_1 = \omega_2/\alpha_2 = \omega_3/\alpha_3$ ($\alpha_1 = 0.203 \text{ mm}^{-1}$, $\alpha_2 = 0.408 \text{ mm}^{-1}$, $\alpha_3 = 0.604 \text{ mm}^{-1}$), which together with the equalities $\omega_2 = 2\omega_1$, $\omega_3 = 3\omega_1$ are the synchronism conditions, are seen to occur exactly for higher harmonics as well as for the subharmonic. The analogical observation was made by Kachanov (1978) with regard to the processing of data obtained in experiments by Kachanov *et al.* (1977). By this means, the presence and amplification of the subharmonic influenced the development of high harmonics in the greater part of the region of disturbance development. Thus, it was found, in the regime with controlled subharmonic priming of frequency $f' = f_1 + \Delta f$, that the harmonics f_2 and f_3 were stationary up to $x = 625 \text{ mm}$, i.e. their amplitudes and phase did not depend on time, whereas the subharmonic parametric resonance appeared and disappeared periodically with a period $T_\Delta = (2\Delta f)^{-1} = 2\text{--}10 \text{ s}$. In the case of a non-controlled priming, the subharmonic amplitude and phase changed in the time in a very complex way (see §3.2), whereas the amplitude and phase of higher harmonics remained practically independent of the time up to $x = 680 \text{ mm}$.

High-harmonic growth curves correspond to those in the work of Kachanov *et al.* (1977) qualitatively. Differences are connected with a difference in the method of measurement of amplitudes of harmonics: in the work of Kachanov *et al.* (1977) the measurements were carried out using maxima in profiles of each of the harmonics (forms of profiles in the present experiment are analogous to those in the experiment of Kachanov *et al.* 1977).

At increasing x , when a three-dimensionality of the fundamental wave is increased (see §3.3), a three-dimensionality of higher harmonics is also increased. Thus, at $x = 600 \text{ mm}$ on some z -sections, the change of z in 2 mm at $y/\delta = 0.26$ could lead to the change of amplitudes of the second and third harmonics in two times and to the change of their phases on π . The process of the generation of three-dimensional higher harmonics plays a great role at the **K**-regime of transition, and, as was mentioned in §3.1, it becomes considerable at larger initial amplitudes of the fundamental wave, when it blocks the process of the resonance excitation of the subharmonic or outruns it.

4.6. Properties of combination modes

The excitation of harmonics with frequencies $f_{\frac{3}{2}} = \frac{3}{2}f_1$ and $f_{\frac{5}{2}} = \frac{5}{2}f_1$, being coherent with a fundamental wave, had been observed both in the regime with a controlled subharmonic priming and without it. However, in the first case the process of the excitation of such harmonics is observed more clearly, and therefore, in this paper, distributions of amplitudes $A_{\frac{3}{2}}$, $A_{\frac{5}{2}}$ and phases $\phi_{\frac{3}{2}}$, $\phi_{\frac{5}{2}}$ versus different coordinates are represented for controlled conditions.

Distributions of phases (in radians of the period $T_1 = 1/f_1$) and amplitudes of combination harmonics are shown in figures 21 and 23(a). Wavevector x -components have the values $\alpha_{\frac{3}{2}} = 0.308 \text{ mm}^{-1}$, $\alpha_{\frac{5}{2}} = 0.510 \text{ mm}^{-1}$, i.e. $\alpha_{\frac{3}{2}} \delta^* = 0.524$,

$\alpha_{\frac{3}{2}}\delta^* = 0.867$, at $x = 600$ mm ($R = 608$). Graphs and given numbers demonstrate again the satisfaction of the synchronism conditions, which is not surprising because combination modes are the result of an interaction of type $f = mf_1 \pm f_{\frac{3}{2}}$, and the existence of the synchronism between mf_1 , $f_{\frac{3}{2}}$ and f_1 was detected early (§§3.2, 4.3 and 4.5).

Unlike harmonics f_2 and f_3 , amplitudes and phases of harmonics $f_{\frac{3}{2}}$ and $f_{\frac{3}{2}}$ depended on the time and oscillated with period $T_{\Delta} = \frac{1}{2}\Delta f$ (where $\Delta f = 0.25 + 0.05$ Hz is the detuning of priming oscillations) on appearance and disappearance of the parametric resonance, the oscillation character coinciding with subharmonic oscillations. Namely, amplitudes $A_{\frac{3}{2}}$ and $A_{\frac{3}{2}}$ varied as $|\cos(\Delta\omega t)|$ in phase with the subharmonic amplitude, and phases $\phi_{\frac{3}{2}}$ and $\phi_{\frac{3}{2}}$ in the region of minimum amplitude changed through 180° by jumps simultaneously with subharmonic phase jumps, being constant between jumps. Such behaviour is natural and connected with the nature of harmonics $f_{\frac{3}{2}}$ and $f_{\frac{3}{2}}$.

Distributions $A_{\frac{3}{2}}(z)$ and $\phi_{\frac{3}{2}}(z)$ at $x = 600$ mm are represented in figure 20. They show a three-dimensionality of fluctuations of frequency $f_{\frac{3}{2}}$, which are mainly like the subharmonic, a pair of oblique waves having approximately the same z -component of the wavevector, $\beta_{\frac{3}{2}} \approx \beta_{\frac{3}{2}} = 0.195$ mm $^{-1}$. The angles of inclination $\theta_{\frac{3}{2}}^{\pm}$ of wavevectors $\mathbf{K}_{\frac{3}{2}}^{\pm}$ to the flow axis differ from those for the subharmonic $\theta_{\frac{1}{2}}^{\pm} : \theta_{\frac{1}{2}}^{\pm} = \pm \arctan(\beta_{\frac{3}{2}}/\alpha_{\frac{3}{2}}) = \arctan 0.633 = 32.3^\circ$.

It should be mentioned that the appearance of the oscillations of frequency $\omega_{\frac{3}{2}}$, with $\beta_{\frac{3}{2}} = \beta_{\frac{1}{2}}$, follows apparently from the interaction of the fundamental wave ($\omega_1, \alpha_1, 0$) with the subharmonics ($\omega_{\frac{1}{2}}, \alpha_{\frac{1}{2}}, \pm\beta_{\frac{1}{2}}$), which gives in terms $O(A_1 A_{\frac{1}{2}})$ the harmonics of ($\omega_1 + \omega_{\frac{1}{2}}, \alpha_1 + \alpha_{\frac{1}{2}}, \pm\beta_{\frac{1}{2}}$) type.

Profiles of the combination mode amplitudes $A_{\frac{3}{2}}(y)$ and $A_{\frac{3}{2}}(y)$ at $x = 600$ mm ($R = 608$) are represented in figure 24. They have two maxima in the wall part of the boundary layer: one maximum is located immediately near the wall at $y/\delta = 0.03$ and another maximum is placed near the subharmonic maximum at $y/\delta = 0.28$. The third maximum is observed in the outer part of the boundary layer.

5. Discussion

5.1. Main conclusions

The process of laminar-flow breakdown is essentially nonlinear and depends critically on outside factors. It compels care to be taken with new experimental (and also theoretical) results in this field. Quite a number of 'anomalous' results on transition are known, some of which were explained by experimental-facility properties or specific conditions of experiments. (The transition reversal in a supersonic boundary layer with deep cooling of the wall is the striking example (see Lysenko & Maslov 1981). This phenomenon proved to be connected closely with humidity of air in wind tunnels and the falling of hoar-frost on the surface.) Therefore it is recognized (see Reshotko 1976; Herbert & Morkovin 1980) that results can be considered as a well established fact if the following conditions are realized. 'Whenever possible, tests should involve more than one facility. Tests should have ranges of overlapping parameters, and whenever possible, experiments should have redundancy in transition measurements' (Reshotko 1976). Morkovin (1978) has extended these stipulations to theoretical researches too, by a 'facility' - meaning a theoretical model with its computer program.

The generation of subharmonics of the Tollmien-Schlichting fundamental wave

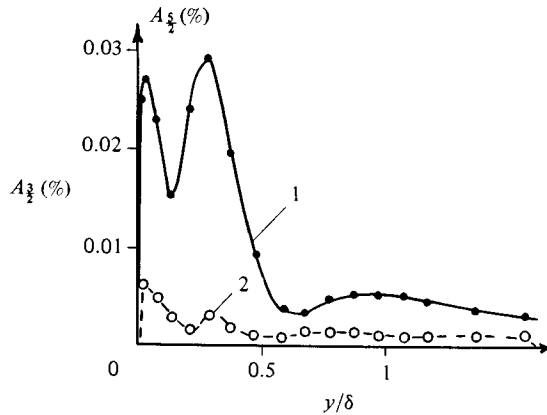


FIGURE 24. y -profiles of amplitudes of oscillations with frequencies $\frac{3}{2}f_1$ (1) and $\frac{5}{2}f_1$ at controlled conditions. $x = 600$ mm ($R = 608$), $z = -2.5$ mm.

and other low-frequency (in comparison with a fundamental wave) disturbances and their important role in the transition process at certain conditions were experimentally derived for the first time by Kachanov *et al.* (1977). In fact, a new path of transition of a laminar boundary to a turbulent one, differing from classical K-breakdown (see Klebanoff *et al.* 1962) in principle, was discovered by them.

Thomas & Saric (1981) and Saric, Carter & Reynolds (1981) have presented visual observations of laminar-turbulent transition in a boundary layer on a flat plate. The experiments were carried out at the same time as the present experiments. The visualization of a picture of laminar-regime breakdown was obtained by means of the smoke-wire method (see Coorke *et al.* 1974) in two different wind tunnels. Two different types of laminar flow breakdown were reported. One type of breakdown was characterized by the presence of a system of Λ -shaped vortices, following one after another with the period of the fundamental wave. Such a picture corresponds to the K-breakdown regime with the formation of typical 'spikes' in the oscilloscope traces, taken in the regions of Λ -shaped vortex tops, and subsequent high-frequency fluctuation splashes (see e.g. Knapp & Roache 1968).

In another case, the period of a one-after-another movement of vortex structures was doubled, which corresponds to oscillations with frequency $\frac{1}{2}f_1$, i.e. to the presence of the subharmonic of the fundamental wave. Thus, in view of the experiments of Kachanov *et al.* (1977), Thomas & Saric (1981), Saric *et al.* (1981) and the present data, *the presence of the subharmonic of the fundamental wave at the laminar-turbulent transition in a boundary layer should be considered as a well-established fact.* Saric *et al.* (1981) have mentioned that the picture corresponding to K-breakdown can be observed at sufficiently large amplitudes of the fundamental wave. The picture corresponding to the presence of the subharmonic was observed at small initial amplitudes of the fundamental wave, the breakdown in this case taking place behind the second branch of the neutral stability curve. These observations coincide with those in Kachanov *et al.* (1977) and the present paper (see §3.1).

The present study was undertaken a few years after the work of Kachanov *et al.* (1977). The same regime of laminar flow breakdown was realized. A fast excitation of the broad spectrum of low-frequency fluctuations, including the subharmonic, with simultaneous appearance of three-dimensionality and following filling of a spectrum by an interaction of low-frequency fluctuations with the fundamental wave and its

harmonics, are the principal features of the present type of transition. No appearance of high-frequency splashes, intermittency and turbulent spots is observed, unlike K-breakdown. In the subsequent stage (stage III of Kachanov *et al.* 1977) a rapid growth of all spectral components takes place, which is accompanied by development of strong three-dimensionality of flow. In this sense, like the case of K-breakdown, it is possible to speak of a catastrophic character of the transition, on a secondary instability. However, in contrast with a high-frequency secondary instability leading to K-breakdown, low-frequency disturbances play the main role in the present case, i.e. it is probably possible to speak of a low-frequency secondary instability. The investigations carried out in the present work showed the cause of the appearance of the low-frequency fluctuation packet to be the parametric resonant excitation of a pair of oblique subharmonic waves by the plane fundamental wave in accordance with the theoretical model of Craik (see Craik 1971; Volodin & Zelman 1978). In the case of a broad spectrum of priming oscillations, the parametric resonance results in an amplification of a rather broad packet of low-frequency oscillations. The spectral width of the packet is connected with the sporadic appearance and disappearance of the resonance in time, which is caused by the change, in time, of the initial conditions for the resonance and results in a modulation of subharmonic amplitude and jumps of subharmonic phase. The three-dimensional nature of resonant subharmonics explains the cause of simultaneous appearance of the three-dimensionality and packet of low-frequency fluctuations in the present type of transition (region II in Kachanov *et al.* 1977).

Thus, because of a stochasticity of priming oscillations in the frequency range $f_i \pm \frac{1}{2}\Delta f_r$ the deterministic process of parametric resonant interaction leads to excitation of the whole packet of three-dimensional low-frequency fluctuations, resulting in the onset of randomization of the disturbance development process. The subsequent interaction of the packet with the fundamental wave and its higher harmonics leads to the filling of the whole spectrum and the complete randomization of the process. These are the main features of the present type of laminar-turbulent transition.

5.2. *Two types of transition: causes of their difference*

What are causes of appearance of the two different types of transition discovered by Klebanoff & Tidstrom (1959) and Kachanov *et al.* (1977)?

The causes of appearance of the K-breakdown regime are discussed in the literature, and different points of view exist (see e.g. Volodin & Zelman 1981; Tani 1981). For the authors of the present paper, Craik's (1971) idea of the excitation, at an initial stage of formation of the K-breakdown regime, of a pair of three-dimensional waves with the fundamental wave frequency ω_1 under the action of a plane wave with the frequency $2\omega_1$ is most attractive. This idea was developed further by Nayfeh & Bozatli (1979*b*), where the interaction of four waves $(\omega_1, \alpha_1, 0)$, $(2\omega_1, 2\alpha_1, 0)$, $(\omega_1, \alpha_1, \pm\beta_1)$ was considered and calculations were applied to the conditions of the experiment of Klebanoff *et al.* (1962). It was considered in this paper that essentially 'two interaction processes [take] place at the same time. The first one is the interaction between a two-dimensional fundamental wave and its second harmonic. As shown by Nayfeh & Bozatli (1979*a*), this is a strong destabilizing mechanism for the second harmonic. In the second part of the interaction, the second harmonic interacts with its two three-dimensional subharmonic waves of order one-half and produces large increases in the amplitudes of the three-dimensional waves.'

It can be supposed on the grounds of the work of Klebanoff *et al.* (1979, 1962) and Nayfeh & Bozatli (1979*b*) that resonant interactions, resulting in an amplification

of different pairs of oblique waves, play an important role at an initial stage of appearance of the K-breakdown regime as well as the regime studied by Kachanov *et al.* (1977) and in the present paper. The transition process, studied by Kachanov *et al.* (1977) ('case 2'), starts with the resonant amplification of a pair of oblique subharmonics from random priming oscillations under the action of a plane fundamental wave. On the other hand, the onset of K-breakdown ('case 1'), to all appearances, is connected with the mechanism described theoretically by Nayfeh & Bozatli (1979*b*) and is caused by the resonance excitation of a pair of oblique waves with a fundamental wave frequency f_1 under the action of the plane harmonic with a frequency $2f_1$, from three-dimensional priming disturbances, generated by a vibrating ribbon on a fundamental frequency f_1 . Therefore the question of which one of our transition regimes will be realized in a concrete case is apparently the same as the question of which of the aforementioned resonances will manifest itself the earlier, or (speaking figuratively) will be 'stronger' and gain victory over the other one.

A resonance 'strength' means the intensity of a pair of resonantly amplified waves (at some point of space), which depends on the amplification rate of resonant waves and the amplitude of priming oscillations. A criterion of the 'victory' in this competition is apparently the reaching by resonantly amplified three-dimensional disturbances of the amplitudes of order an amplitude of the fundamental wave A_1 , when the strong nonlinear interaction of waves begins, the advantages of one type of resonance being simultaneously the defects of the other one.

In the first case, i.e. at realization of the K-breakdown regime, a large amplitude of priming oscillations is the main advantage, because these oscillations have the frequency of a fundamental wave. The main defect of resonance in this case consists in the fact that the amplitude of the second harmonic A_2 , which excites oblique waves with amplification rates proportional to A_2 , is not very large in comparison with the amplitude of the fundamental wave.

In contrast, in the second case, i.e. at subharmonic excitation, resulting in the second type of transition, a large amplitude of a plane forcing wave, which coincides here with a fundamental wave, is the main advantage, which ensures large amplification rates of the subharmonics. However, the excitation begins from background priming oscillations with very small amplitudes, which require large distances in space for their sufficient amplification.

Strictly speaking, under priming oscillations only those disturbances are meant for which the synchronism conditions (4) are realized. A wave spectrum of initial oscillations in the resonance band contains mainly the plane waves ($\beta \approx 0$) both in the first case and, apparently, in the second (see §4.3). However, in view of the finite length of a vibrating ribbon, a broad spectrum of oscillations with $\beta \neq 0$ is present in this spectrum. This spectrum contains, in particular, the waves for which the synchronism conditions are also realized (at $\theta \approx 60^\circ$).

In the light of the aforesaid, it is clear why the first regime of transition appeared, in the works of Kachanov *et al.* (1977) and Saric *et al.* (1981) and in the present experiments, when the amplitude of vibrating-ribbon oscillations was increased, and why the appearance of the second regime was observed at smaller amplitudes. On increasing A_1 , the intensity of a forcing wave exciting the subharmonic (case 2) increases, but the value of the priming remains constant. On increasing A_1 in the first case, the amplitude of a forcing wave A_2 (the amplitude of the harmonic $2f_1$) increases faster than A_1 because the term responsible for pumping of energy from f_1 to $f_2 = 2f_1$ is proportional to A_1^2 (see e.g. Nayfeh & Bozatli 1979*b*). Simultaneously with

the growth of A_1 , the intensity of the priming, in the first case, also increases, although it was large without that. Moreover, it was detected by the authors of the present paper that, on increasing the ribbon oscillation amplitude, the width of a wave packet on a frequency f_1 increases owing to an amplification of small-scale (in comparison with the ribbon length) non-uniformity on z (a large β). These non-uniformities are apparently connected with some z -non-uniformities of the ribbon form (local attack angles, bending, etc.) and the value of the magnetic field. The detected phenomenon also contributes to increase of priming disturbances in the first case and its prevalence over the second one increasing the signal fed to the ribbon.

For existence of a parametric resonant amplification, realization of the condition of a favourable initial phase for priming oscillations is necessary, besides realization of the synchronism condition. This condition leads to the importance of a component of oscillations on a frequency of the excited wave, having a phase ϕ_r relative to the forcing wave. It is very important in the first case. Then the value of the resonant component is proportional to $\cos(\phi_2 - \phi_r)$, where ϕ_2 is a phase shift between the fundamental wave and a wave with the frequency $2f_1$ excited by a harmonic resonance. Apparently the K-breakdown regime would not appear even at very large amplitudes of a fundamental wave in the hypothetical case $\phi_2 = \phi_r + \frac{1}{2}\pi$. However, because of a dependence of flow parameters on R , this condition can be realized only at one point because $\cos(\phi_2 - \phi_r) \neq 0$ downstream, and the resonance can take place all the same (see §4.1). It should be noted that amplitude A_2 and phase ϕ_2 of the second harmonic depend only on parameters of a flow and a fundamental wave (R, F_1, A_1) and do not depend on background priming disturbances with frequency $2f_1$, if their intensity is sufficiently small. In the second case the condition of resonant excitation $\phi_{\frac{1}{2}} - \phi_1 = \phi_r$ results in the singling out, from a continuous spectrum of priming oscillations, a wave packet of frequency bandwidth $f_1 \pm \frac{1}{2}\Delta f_r$, with wave phases having the definite properties studied in §3.4.

In conclusion it should be mentioned that, apparently, three-wave resonant interactions play a very important role in the subsequent development of K-transition. It was noted in Kachanov *et al.* (1982) that the excitation of harmonics $n\omega_1$ ($n = 2, 3, \dots$) is characteristic of the K-regime in well-controlled conditions, amplitudes of these harmonics, when 'spikes' appear, reaching values close to the amplitudes of a fundamental wave. With these conditions, besides the resonance of Nayfeh & Bozatlı's (1979*b*) type, all conditions for resonances $(2n\omega_1, \alpha_{2n}, 0) \rightarrow (n\omega_1, \frac{1}{2}\alpha_{2n}, \pm\beta_n)$, where $n = 2, 3, 4, \dots$, arise. Pairs of three-dimensional waves $\pm\beta_n$ with frequencies $n\omega_1$ can amplify as a result of these resonances. Because of strong resonant linkage of disturbances in such triads, their development can be probably considered, in first approximation, independently. Apparently, just the simultaneous nonlinear amplification of two-dimensional harmonics and appearance of the above set of three-wave resonances result in, at superposition, formation of the typical, t - and z -periodical, nonlinear system of waves with z -peaks and t -spikes which is typical for an definite stage of K-breakdown.

The authors are indebted to Dr M. B. Zelman and I. I. Maslennikova for imparting the results of their calculations. We would also like to acknowledge valuable discussions with Prof. W. S. Saric.

Appendix. A remark on interpretation of the experimental data

All experimental data of this paper were obtained by the use of a single-wire probe and related only to the longitudinal components of velocities. Main attention was concentrated on the elucidation of the nature of the subharmonic, and it was proved that the excitation of the subharmonic has a resonant character. All data on the amplification of the low-frequency packet of waves are explained in terms of the resonant amplification of the oblique symmetric subharmonics having some sufficiently broad spectral width of the resonance. The effective resonance within the symmetric triad of waves at sufficiently large values of detunings from conditions of exact resonance is corroborated by calculations (Zelman & Maslennikova 1982). However, the data on the excitation of a low-frequency disturbance packet with some distinct peaks can suggest the existence of some other, non-symmetric, resonant triads of the type

$$(\alpha_1, 0, \omega_1), \quad (\alpha_2, \pm\beta, \omega_2), \quad (\alpha_1 - \alpha_2, \mp\beta, \omega_1 - \omega_2). \quad (\text{A } 1)$$

Indeed, all results on excitation of low-frequency oscillations can be treated in the language of resonant triads of type (A 1) as well as on the language of symmetric subharmonic triads. Using simple transformations, it is not difficult to show that both interpretations are absolutely equivalent.

Let us redesignate in (A 1):

$$\alpha_1 = 2\alpha_2, \quad \alpha_2 = \alpha_2 + \Delta\alpha, \quad \beta = \beta_2, \quad \omega_1 = 2\omega_2, \quad \omega_2 = \omega_2 + \Delta\omega,$$

i.e. the resonant triads (A 1) will be

$$(2\alpha_2, 0, 2\omega_2), \quad (\alpha_2 + \Delta\alpha, \pm\beta_2, \omega_2 + \Delta\omega), \quad (\alpha_2 - \Delta\alpha, \mp\beta_2, \omega_2 - \Delta\omega). \quad (\text{A } 2)$$

Assuming the parallel approximation, i.e. independence of the form of eigenfunctions on x -coordinate, four waves, forming two pairs of oblique waves in triads (A 2), can be presented in the form

$$\left. \begin{aligned} u_1(x, y, z, t) &= C_1 A^{(1)}(y) e^{i\delta^{(1)}(y)} e^{-\alpha^{(1)}(x-x_0)} e^{i[(\alpha_2 + \Delta\alpha)x - (\omega_2 + \Delta\omega)t + \beta_2 z + \theta_1]}, \\ u_2(x, y, z, t) &= C_2 A^{(1)}(y) e^{i\delta^{(1)}(y)} e^{-\alpha^{(1)}(x-x_0)} e^{i[(\alpha_2 + \Delta\alpha)x - (\omega_2 + \Delta\omega)t - \beta_2 z + \theta_2]}, \\ u_3(x, y, z, t) &= C_3 A^{(2)}(y) e^{i\delta^{(2)}(y)} e^{-\alpha^{(2)}(x-x_0)} e^{i[(\alpha_2 - \Delta\alpha)x - (\omega_2 - \Delta\omega)t - \beta_2 z + \theta_3]}, \\ u_4(x, y, z, t) &= C_4 A^{(2)}(y) e^{i\delta^{(2)}(y)} e^{-\alpha^{(2)}(x-x_0)} e^{i[(\alpha_2 - \Delta\alpha)x - (\omega_2 - \Delta\omega)t + \beta_2 z + \theta_4]}. \end{aligned} \right\} \quad (\text{A } 3)$$

Here C_i ($i = 1, 2, 3, 4$) are the initial amplitudes of the waves (in the region of the resonance), $A^{(j)} e^{i\delta^{(j)}(y)}$ are complex functions of y -distributions of amplitudes and phases of waves u_1, u_2 ($j = 1$) and u_3, u_4 ($j = 2$), $\alpha_i^{(j)}$ ($j = 1, 2$) are spatial amplification rates (they are equal to the sum of the linear amplification rates and the increment of parametric amplification), and θ_i ($i = 1, 2, 3, 4$) are initial phases of waves u_i . Wave-vectors of (A 3) are represented in figure 25.

Apparently, we can make the formal addition of the wave u_1 with u_4 and u_2 with u_3 , having obtained a pair of symmetric waves of the type

$$\left. \begin{aligned} u^+(x, y, z, t) &= D^+(x, y, t) e^{i[\alpha_2 x + \beta_2 z - \omega_2 t + \theta^+(x, y, t)]}, \\ u^-(x, y, z, t) &= D^-(x, y, t) e^{i[\alpha_2 x - \beta_2 z - \omega_2 t + \theta^-(x, y, t)]}. \end{aligned} \right\} \quad (\text{A } 4)$$

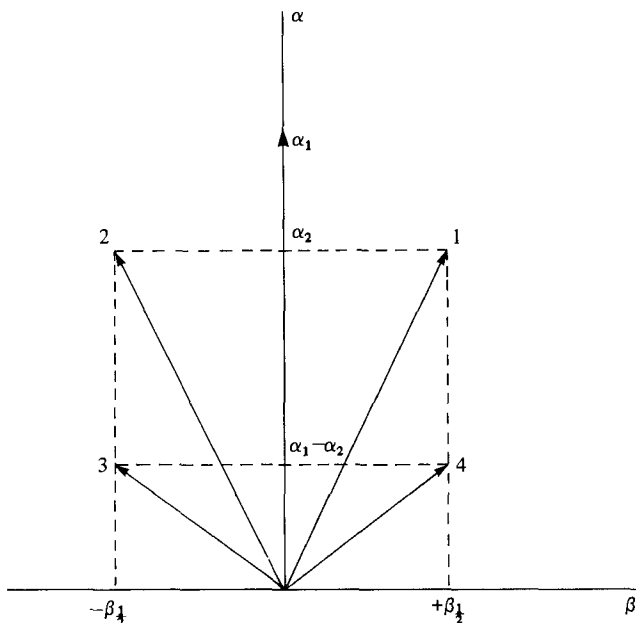


FIGURE 25. Wavevectors of (A 3).

We have here

$$D^+(x, y, t) = \{[D_1(x, y)]^2 + [D_4(x, y)]^2 + 2D_1(x, y)D_4(x, y)\cos[\delta^{(1)}(y) + \theta_1 - \delta^{(2)}(y) - \theta_4 + 2\Delta\alpha x - 2\Delta\omega t]\}^{\frac{1}{2}},$$

$$\tan \theta^+(x, y, t) = \frac{D_1 \sin[\delta^{(1)} + \theta_1 + \Delta\alpha x - \Delta\omega t] + D_4 \sin[\delta^{(2)} + \theta_4 - \Delta\alpha x + \Delta\omega t]}{D_1 \cos[\delta^{(1)} + \theta_1 + \Delta\alpha x - \Delta\omega t] + D_4 \cos[\delta^{(2)} + \theta_4 - \Delta\alpha x + \Delta\omega t]},$$

$$D_i(x, y) = |u_i(x, y, z, t)| \quad (i = 1, 2, 3, 4),$$

and the corresponding formulae for $D^-(x, y, t)$ and $\theta^-(x, y, t)$. The main thing in (A 4) is x - and t -modulation of amplitudes and phases.

Then the formal sum of waves (A 4) gives

$$u(x, y, z, t) = D(x, y, z, t) e^{i[\alpha_1 x - \omega_1 t + \theta(x, y, z, t)]}, \quad (\text{A } 5)$$

i.e. a plane wave with an amplitude and a phase, as the corresponding formulae show, modulated on x , z and t . Just such a summed signal is fixed by the probe of the hot-wire anemometer, and it can be interpreted in principle in terms of (A 5) as well as of (A 4) or (A 3).

However, in order that the experimental data of this paper might be treated in terms of (A 3), these waves must have some special properties besides the fact that they are resonant triads with the wave $(\alpha_1, 0, \omega_1)$.

First, the amplitude of the subharmonic in the experiments depended on z as $|\cos(\beta_{\frac{1}{2}} z)|$, and its phase was constant on z within the jumps on π : It can be found from formulae for the amplitudes and the phases in (A 5) that

$$D(x, y, z, t) = D'(x, y, t) \cos(\beta_{\frac{1}{2}} z + \Delta\theta),$$

$$\theta(x, y, z, t) = \theta'(x, y, t)$$

when the amplitudes of u_1 and u_2 are equal, those of u_3 and u_4 are equal and the phase differences $\theta_1 - \theta_2 = \theta_4 - \theta_3 \equiv 2\Delta\theta$.

Secondly, it has been emphasized more than once in this paper that the phase of the subharmonic in the experiments did not depend on the time (within jumps on π), this fact being established with the utmost care. For the waves (A 3) to correspond to this observation, equalities of amplitudes of u_1 and u_4 , amplitudes of u_2 and u_3 and phase differences $\theta_1 - \theta_4$ and $\theta_2 - \theta_3$ are necessary. These equalities also eliminate beats on x .

On realization of the aforesaid conditions (obviously, they are realized in this experiment) resonantly amplified subharmonic oscillations, observed in the experiments, can be treated either as the pair of symmetric oblique subharmonics (A 4) (as in this paper) or as two non-symmetric pairs of waves of type (A 3), or as one plane wave of type (A 5).

The aforesaid is concerned with the interpretation of experiments with a controlled priming subharmonic. In the case of non-controlled initial subharmonic oscillations it is possible to carry out analogous manipulations using a superposition of quartets of waves of type (A 3) with different detunings $\Delta\omega$ (and $\Delta\alpha$). As a result we will have some conditions when the observed experimental data may with equal reason be treated by any of the above techniques.

It should be mentioned that the equality of amplitudes of the subharmonics within a symmetric triad of type (A 4), corresponding to observed experimental facts (figure 8), is in itself the effect of three-wave resonant interaction. This is also corroborated by calculations (Zelman & Maslennikova, 1982).

In conclusion it can be noted that the interpretation of the experimental data by different but not incompatible approaches is a matter of convenience to a certain degree. Different views on experimental data may sometimes lead to the revealing of interesting physical phenomena (see e.g. Miksad *et al.* 1982).

REFERENCES

- BETCHOV, R. 1960 On the mechanism of turbulent transition. *Phys. Fluids* **3**, 1026.
- COORKE, T., KODA, D., DRUBKA, R. & NAGIB, H. 1974 A new technique for introducing controlled sheets of smoke streaklines in wind tunnels. In *Proc. Intl Congr. Instrum. Aerospace Simulation Facilities; IEEE Publ.* 77 CH 1251-8 AES, p. 74.
- CRAIK, A. D. 1971 Non-linear resonant instability in boundary layers. *J. Fluid Mech.* **50**, 393.
- CRAIK, A. D. 1980 Nonlinear evolution and breakdown in unstable boundary layers. *J. Fluid Mech.* **99**, 247.
- EPPLER, R. & FASEL, H. (ed.) 1980 *Laminar-Turbulent Transition*. Springer.
- FREYMUTH, P. 1966 On transition in a separated laminar boundary layer. *J. Fluid Mech.* **25**, 683.
- GERTSENSHTEIN, S. YA. 1969 On stability of a nonstationary unidirectional parallel flow of ideal liquid. *Izv. Akad. Nauk SSSR, Mekh. Zhidk. i Gaza* **2**, 5 (in Russian).
- GILYOV, V. M., KACHANOV, YU. S. & KOZLOV, V. V. 1981 A development of a space wave packet in a boundary layer. *Preprint N34, Novosibirsk, ITPM SO AN SSSR* (in Russian).
- GREENSPAN, H. P. & BENNEY, D. J. 1963 On shear-layer instability, breakdown and transition. *J. Fluid Mech.* **15**, 133.
- HAMA, F. R. & NUTANT, J. 1963 Detailed flow observation in the transition process in a thick boundary layer. In *Proc. Heat Transfer and Fluid Mech. Inst.*, p. 77. Stanford University Press.
- HERBERT, T. & MORKOVIN, M. V. 1980 Dialogue on bridging some gaps in stability and transition research. In Eppler & Fasel (1980), p. 47.
- ITOH, N. 1981 Secondary instability of laminar flows. *Proc. R. Soc. Lond. A* **375**, 565.
- KACHANOV, YU. S. 1978 Experimental modelling of laminar-turbulent transition in a boundary layer. Dissertation, ITPM SO AN SSSR, Novosibirsk (in Russian).
- KACHANOV, YU. S., KOZLOV, V. V. & LEVCHENKO, V. YA. 1974 Experimental investigation of the influence of cooling on the stability of laminar boundary layer. *Rep. Siberian Div. Acad. Sci. USSR* **8**, 75 (in Russian).

- KACHANOV, YU. S., KOZLOV, V. V. & LEVCHENKO, V. YA. 1975 A development of small amplitude oscillations in laminar boundary layer. *Sci. Ann. of TsAGI* **6**, 137 (in Russian).
- KACHANOV, YU. S., KOZLOV, V. V. & LEVCHENKO, V. YA. 1977 Nonlinear development of a wave in a boundary layer. *Izv. Akad. Nauk SSSR, Mekh. Zhidk. i Gaza* **3**, 49 (in Russian). (See also *Fluid Dyn.* **12** (1978), 383).
- KACHANOV, YU. S., KOZLOV, V. V. & LEVCHENKO, V. YA. 1980 Experiments on nonlinear interaction of waves in boundary layer. In Eppler & Fasel (1980), p. 135.
- KACHANOV, YU. S., KOZLOV, V. V. & LEVCHENKO, V. YA. 1982 *Beginning of Turbulence in a Boundary Layer*. Novosibirsk, Nauka (in Russian).
- KLEBANOFF, P. S. & TIDSTROM, K. D. 1959 Evolution of amplified waves leading to transition in a boundary layer with zero pressure gradient. *NACA TN D-195*.
- KLEBANOFF, P. S., TIDSTROM, K. D. & SARGENT, L. M. 1962 The three-dimensional nature of boundary-layer instability. *J. Fluid Mech.* **12**, 1.
- KNAPP, C. F. & ROACHE, P. J. 1968 A combined visual and hot-wire anemometer investigation of boundary-layer transition. *AIAA J.* **6**, 29.
- KOMODA, H. 1967 Nonlinear development of disturbance in the laminar boundary layer. *Phys. Fluids Suppl.* **10**, S87.
- KORN, G. A. & KORN, T. M. 1961 *Mathematical Handbook for Scientists and Engineers*. McGraw-Hill.
- KOVASZNAVY, L. S., KOMODA, H. & VASUDEVA, B. R. 1962 Detailed flow field in transition. In *Proc. Heat Transfer and Fluid Mech. Inst.*, p. 1. Stanford University Press.
- KOSLOV, V. V. & RAMAZANOV, M. P. 1981 Experimental investigation of Poiseuille flow stability. *Rep. Siberian Div. Acad. Sci. USSR* **8**, 45 (in Russian).
- LANDAHL, M. T. 1972 Wave mechanics of breakdown. *J. Fluid Mech.* **56**, 775.
- LYSENKO, V. I. & MASLOV, A. A. 1981 Transition reversal and one of its causes. *AIAA J.* **19**, 705.
- MIKSAD, R. W. 1972 Experiments on the non-linear stages of free-shear-layer transition. *J. Fluid Mech.* **56**, 695.
- MIKSAD, R. W. 1973 Experiments on nonlinear interactions in the transition of a free shear layer. *J. Fluid Mech.* **59**, 1.
- MIKSAD, R. W., JONES, F. L., POWERS, E. L., KIM, Y. C. & KHADRA, L. 1982 Experiments on the role of amplitude and phase modulations during transition to turbulence. *J. Fluid Mech.* **123**, 1.
- MORKOVIN, M. V. 1978 Instability, transition to turbulence and predictability. *AGARD-AG-236*.
- NAYFEH, A. H. & BOZATLI, A. N. 1979a Nonlinear interaction of waves in boundary-layer flows. *VPI & SU Rep.* NVPI-E-79.6.
- NAYFEH, A. H. & BOZATLI, A. N. 1979b Nonlinear wave interactions in boundary layers. *AIAA Paper* N79-1493.
- NISHIOKA, M., IIDA, S. & ISHIKAWA, Y. 1975 An experimental investigation of the stability of plane Poiseuille flow. *J. Fluid Mech.* **72**, 731.
- RABINOVICH, M. I. 1978 Stochastic autooscillations and a turbulence. *Usp. Fiz. Nauk* **125**, 123 (in Russian).
- RAETZ, G. S. 1959 *Northrop Rep.* NOR-59,383 (BLC-121) (see also Stuart 1960).
- RESHOTKO, E. 1976 Boundary-layer stability and transition. *Ann. Rev. Fluid Mech.* **8**, 311.
- ROSS, J. A., BARNES, F. H., BURNS, J. G. & ROSS, M. A. S. 1970 The flat plate boundary layer. Part 3. Comparison of theory with experiment. *J. Fluid Mech.* **43**, 819.
- SARIC, W. S., CARTER, J. D. & REYNOLDS, G. A. 1981 Computation and visualization of unstable-wave streamlines in a boundary layer. *Bull. Am. Phys. Soc.* **26**, 1252.
- SARIC, W. S. & NAYFEH, A. H. 1975 Non-parallel stability of boundary-layer flows. *VPI & SU Rep.* VPI-E-75-5.
- SARIC, W. S. & REYNOLDS, G. A. 1980 Experiments on the stability of nonlinear waves in a boundary layer. In Eppler & Fasel (1980), p. 125.
- SATO, H. 1960 The stability and transition of two-dimensional jet. *J. Fluid Mech.* **7**, 53.
- SATO, H. & KURIKI, K. 1961 The mechanism of transition in the wake of a thin flat plate placed parallel to a uniform flow. *J. Fluid Mech.* **11**, 321.
- SCHUBAUER, G. B. & SKRAMSTAD, H. K. 1947 Laminar boundary layer oscillations and stability of laminar flow. *J. Aerospace Sci.* **14**, N2.

- STUART, J. T. 1960 Non-linear effects in hydrodynamic stability. In *Proc. 10th Intl Congr. Appl. Mech., Stresa, Italy*, pp. 91–97. Elsevier.
- TANI, J. & KOMODA, H. 1962 Boundary-layer transition in the presence of streamwise vortices. *J. Aerospace Sci.* **29**, N4.
- TANI, I. 1981 Three-dimensional aspects of boundary-layer transition. *Proc. Indian Acad. Sci. (Engng Sci.)* **4**, 219.
- THOMAS, A. S. W. & SARIC, W. S. 1981 Harmonic and subharmonic waves during boundary-layer transition. *Bull. Am. Phys. Soc.* **26**, 1252.
- VOLODIN, A. G. & ZELMAN, M. B. 1978 Three-wave resonance interaction of disturbances in a boundary layer. *Izv. Akad. Nauk SSSR, Mekh. Zhidk i Gaza* **5**, 78 (in Russian).
- VOLODIN, A. G. & ZELMAN, M. B. 1981 The nature of differences in some forms of transition in the boundary layer. *ALAA J.* **19**, 950.
- WHITHAM, G. B. 1974 *Linear and Nonlinear Waves*. Wiley.
- ZELMAN, M. B. 1981 A development of disturbances with finite amplitudes in plane flows. *Preprint N10, Novosibirsk, ITPM SO AN SSSR* (in Russian).
- ZELMAN, M. B. & MASLENNIKOVA, I. I. 1982 IN *Instability of Sub- and Supersonic Flows* (ed. V. Ya. Levchenko), pp. 5–15. ITPM SO AN SSSR, Novosibirsk (in Russian).
- ZHIGULYOV, V. N., KIRKINSKIY, A. N., SIDORENKO, N. V. & TUMIN, A. M. 1976 On a mechanism of secondary instability and its role in a process of turbulence beginning. In *Aerodynamics*. Moscow, Nauka (in Russian).